

FINAL PERFORMANCE REPORT

As Required by

THE ENDANGERED SPECIES PROGRAM

TEXAS

Grant No. TX ET-149-R

F14AP00853

Endangered and Threatened Species Conservation

Age, growth and environmental exposure histories of threatened freshwater mussels assessed with sclerochronology and shell stable isotopes

Prepared by:

Dr. Bryan Black and Dr. Benjamin Walther



Carter Smith
Executive Director

Clayton Wolf
Director, Wildlife

10 November 2017

FINAL PERFORMANCE REPORT

STATE: Texas **GRANT NUMBER:** TX ET-149-R

GRANT TITLE: Age, growth and environmental exposure histories of threatened freshwater mussels assessed with sclerochronology and shell stable isotopes.

REPORTING PERIOD: 1 September 2014 to 31 August 2017

OBJECTIVE(S): To assess age, long-term growth patterns, and relationships to climate in two threatened mussels, golden orb and Texas pimpleback, using sclerochronology and shell stable isotopes.

Segment Objectives:

Task 1. Shell collection (Winter 2013). Samples of live golden orb and Texas pimpleback are readily collected in conjunction with Texas Parks and Wildlife (TPWD) mussel surveys. If necessary, additional shells could be collected in 2014 to supplement prior collections.

Task 2. Shell processing (Fall-Winter 2014). Shells will be cleaned and sectioned for age and growth analysis. A thin section will be removed for age and growth analyses (chronology development) while an adjacent thick section containing the same increments will be removed for stable isotope analyses.

Objective 3. Age and growth (Winter 2014-Spring 2015). Growth increments will be analyzed in thin-sectioned mussel shells.

Significant Deviations: None.


Summary Of Progress: See Attachment A.

Location: UT Marine Science Institute, Port Aransas, TX.

Cost: Costs were not available at time of this report.

Prepared by: Craig Farquhar

Date: 10 November 2017

Approved by:  **Date:** 10 November 2017

C. Craig Farquhar

ATTACHMENT A

Age, growth, and environmental exposure histories of threatened freshwater mussels assessed with sclerochronology and shell stable isotopes.

Dr. Benjamin Walther
Assistant Professor, Department of Life Sciences
Texas A&M University - Corpus Christi
6300 Ocean Drive
Unit # 5858
Corpus Christi, Texas 78412
benjamin.walther@tamucc.edu; 361-825-4168

Dr. Bryan Black
Associate Professor, Department of Marine Science
Marine Science Institute, University of Texas at Austin
750 Channel View Drive
Port Aransas, TX 78373
bryan.black@utexas.edu; 361-749-6789

Abstract

Texas freshwater mussels are vulnerable to habitat loss and alteration due to river impoundments, dewatering, and climate shifts. Yet despite the precipitous decline of mussel abundances across the state and the urgent need to identify appropriate conservation strategies, little is known about the basic biology of some of the most vulnerable species. Here, we apply growth-increment analysis to two threatened freshwater mussel species, the golden orb *Quadrula aurea* and Texas pimpleback *Quadrula petrina* to provide basic age and growth information and also address questions of environmental tolerances and responses to environmental variability. Twenty-two *Q. petrina* and ten *Q. aurea* individuals were live collected from the Guadalupe River and the shells thin sectioned for growth-increment analysis. For both species growth increments were indistinct and difficult to identify, though they were somewhat more clearly delineated in *Q. petrina* relative to *Q. aurea*. All individuals were quite young in age, establishing after 2007 with the vast majority were less than five years in age. *Q. petrina* did appear to have episodic recruitment with a large pulse in 2011 to which half the sample dates, which may suggest some environmental control on reproduction in this species. Time series of carbon and oxygen isotope ratios across shell growth increments were investigated for seasonal and yearly patterns to assess their ability to cross-validate age assignments. Isotope ratios did not indicate clear seasonal patterns, likely due to variable increment spacing and inconsistencies in the number of subsamples obtained per year. Annual patterns in average isotope values were then compared with temperature and river discharge metrics. Relationships between $\delta^{18}\text{O}$ and $\delta^{13}\text{C}$ and average monthly air temperature by year were negative, as expected, although only the relationship between $\delta^{13}\text{C}$ and air temperature was significant. Relationships between isotopes and various discharge metrics were not significant. Isotopes were thus of limited utility in confirming assigned ages or reconstructing seasonal environmental experiences. Future work employing isotopes in these species will require higher resolution sampling to discern seasonal patterns.

Objective

To assess age, long-term growth patterns, and relationships to climate in two threatened mussels, golden orb and Texas pimpleback, using sclerochronology and shell stable isotopes.

Introduction

As a group, freshwater mussels are thought to be slow growers with long lifespans. Many Unionidae species living several decades and some with mean ages of 50+ years (Strayer et al., 2004). Although age and growth curves for mussels have been made using von Bertalanffy equations, these methods can significantly deviate from true size-at-age relationships (Haag, 2009). The tree-ring technique of “crossdating,” in which synchronous growth patterns induced by climate are matched among individuals from a given species and site provides much more accurate results (Rypel et al. 2008, 2009, Black et al. 2010). Growth-increment widths can also be measured to develop an exactly dated chronology of population-wide growth anomalies, which can be compared to instrumental records of temperature and discharge to establish climate-growth relationships. Crossdating and chronology (i.e. “sclerochronology”) approaches have been successful with freshwater mussels in other regions of the Southeast (Rypel et al., 2008; Rypel et al., 2009) and underscore the sensitivity of growth to freshwater discharge. Similarly strong negative relationships between freshwater mussel growth and discharge have also been described for long-lived *Margaritifera* and *Gonidea* species of the Pacific Northwest (Black et al. 2010, Black et al. 2015).

In addition to needing basic age and growth information, there are a range of questions about mussel environmental tolerances and responses to altered environmental conditions. One of the most serious threats to mussel populations is altered streamflow dynamics due to impoundments, with dewatering and severe drought events exacerbating stressful conditions (Strayer et al. 2004). Mussels are known to have temperature-dependent reproduction and glochidial release rates, and extreme high or low temperatures can disrupt these processes (Strayer 2008). A particular concern is whether mussels living below impoundments suffer reduced growth and reproductive rates following punctuated releases of cold water from the depths of upstream reservoirs.

One effective way to reconstruct temperature histories is by analyzing the oxygen isotopic composition of bivalve shells, which strongly reflect ambient water conditions as modified by temperature. Stable isotope ratios in biogenic carbonates such as shells of bivalves can be effective proxies for environmental conditions at the time of accretion (Sharp 2007, Cusack and Freer 2008). This is because a variety of abiotic and biotic factors affect uptake and fractionation of isotopes of a given element in specific ways. Two of the most frequently employed carbonate isotope ratios are $\delta^{18}\text{O}$ and $\delta^{13}\text{C}$, primarily for their utility as thermometers (Druffel 1997, Surge et al. 2001, Corrège 2006, Gillikin et al. 2006, McConnaughey and Gillikin 2008). Ratios of $\delta^{18}\text{O}$ in carbonates are primarily driven by two factors: (1) source water $\delta^{18}\text{O}$ ratios and (2) temperature (Sharp 2007). Assuming source water composition is constant, temperature-driven equilibrium

fractionation between water and carbonate leads to an inverse relationship between temperature and carbonate $\delta^{18}\text{O}$. However, water $\delta^{18}\text{O}$ composition is not always constant, particularly in environments dominated by evaporation that causes fractionation and shifts in the source water ratios. Temperature records are extremely limited in freshwater systems. Thus, these isotopes can therefore give great insight into the range of temperatures experienced by individual mussels and their effects on growth trajectories.

Ratios of $\delta^{13}\text{C}$ in biogenic carbonates such as mollusk shells are primarily driven by two factors as well: (1) ambient dissolved inorganic carbon (DIC) ratios and (2) “vital effects” consisting of metabolic alteration of the internal DIC pool and kinetic fractionation (McConnaughey et al. 1997). Any process that alters ambient DIC $\delta^{13}\text{C}$ ratios should be reflected in accreted carbonate $\delta^{13}\text{C}$ ratios. For instance, temporal or spatial shifts in ecosystem metabolism from net production to net respiration can result in variable estuarine DIC $\delta^{13}\text{C}$ ratios and therefore carbonate values (Oczkowski et al. 2010). In contrast to oxygen isotopes, metabolic activity may alter internal DIC pools enough to shift carbonate $\delta^{13}\text{C}$ ratios out of equilibrium with ambient DIC. Traditionally, researchers assumed that bivalve shells precipitated in or near isotopic equilibrium, with minimal metabolic contribution (McConnaughey et al. 1997, McConnaughey and Gillikin 2008). Recently, however, some investigators have measured metabolic contributions as high as 35-37% for some bivalves (Gillikin et al. 2007, Gillikin et al. 2009). These simultaneously operating internal and external dynamics can pose challenges for interpreting isotopic time series. However, if the external and environmental signals are large relative to internal modifications, these isotopic time series in bivalve shells can still be used to reconstruct environmental histories. Indeed, the isotopic composition bivalve shell increments has been successfully applied as a means by which to reconstruct environmental conditions in unionids in Europe (Versteegh et al. 2011), and thus may be relevant to address similar issues elsewhere.

In Texas, freshwater mussels are vulnerable to habitat loss and alteration due to river impoundments, dewatering, and climate shifts (Burlakova et al., 2011). Currently, 5 native Texas mussels are candidates for listing under the Endangered Species Act (ESA) as well as being listed as Threatened at the State level. However, despite the precipitous decline of mussel abundances across the State and the urgent need to identify appropriate management strategies to conserve populations, little is known about the basic biology of some of the most threatened species. Currently, no species-specific age and growth information exists for any of the 5 ESA candidate species, including golden orb and Texas pimpleback. These basic yet critical data are essential for any assessment of demographic shifts, recruitment dynamics, and population sustainability in the face of natural and anthropogenic change. Similarly, although the influences of streamflow and

temperature fluctuations are known to have important lethal and sublethal consequences on mussels, little direct information is known about the temperature and streamflow tolerances of these threatened species. Thus, the objectives of this study are to apply state of the art isotope and growth-increment analyses borrowed from the tree-ring sciences to i) establish mussel ages and ii) quantify relationships between mussel growth and environmental variability, including river discharge and water temperature for two threatened freshwater mussel species in central Texas. Here, we apply these techniques to two threatened species, the golden orb *Quadrula aurea* and Texas pimpleback *Quadrula petrina*. This project serves as a pilot study to evaluate the effectiveness of the proposed methods in Texas, which could subsequently be broadly applied to these and other freshwater mussels across the State.

Methods

Two species of freshwater mussels were collected (*Quadrula petrina*; n = 31 and *Quadrula aurea*; n = 40) on 29 July 2015 in the Guadalupe River south of Hwy 183 in Gonzales, TX (29°29'2.77"N, 97°26'54.62"W) at a location downstream of the confluence with the San Marcos river. Only live-collected specimens were kept so that a known date to the most recently accreted exterior increment. All specimens (10 *Q. aurea*; and 21 *Q. petrina*) were cleaned and embedded in epoxy, thin sectioned to approximately 1 mm thickness on a Buehler IsoMet saw, mounted on slides, and then polished with 10 µm and then 9 µm lapping film. Thin sections were viewed at approximately 20 x magnification with transmitted light and photographed using a binocular Leica Mz microscope and DFC digital camera.

If mussels are sufficiently long-lived, growth increments can be crossdated among individuals to yield the highest data quality possible. Crossdating is one of the central principles of dendrochronology (tree-ring science), and is based on the assumption that environmental factors limit growth, thereby inducing synchronous growth patterns or 'bar codes' that can be visually matched among individuals within a given population and region (Douglass 1941). If an increment was accidentally missed or falsely added, the growth pattern in that individual would be offset by a year relative to the other individuals in the sample set, indicating that a possible error had occurred. However, a dating correction was only made if the error could be confirmed by carefully re-inspecting otolith structure for a micro-increment, false increment, or other aberration. By applying crossdating, the correct calendar year of formation can be assigned to each growth increment, ensuring that high-frequency variability is fully captured in the final biochronology (Black et al. 2016).

Once all samples were visually crossdated, increment widths were measured continuously along the axis of growth and thus perpendicular to each annual increment boundary using Image-

Pro Premier v.9.1 (Media Cybernetics, Silver Spring, Maryland, USA). All increments were measured in the prismatic layer. If measurement time series are sufficiently long (> 15 yr), a growth-increment chronology can be developed by fitting each measurement time series with a negative exponential function and then dividing observed increment widths by those predicted. The resulting standardized growth-increment values can then be averaged with respect to calendar year to yield the chronology for which any value greater than one indicates above-average population-level growth and any value below one indicated below-average population-level growth.

After increment analysis, thin cross-sections of shells from five different individuals per species (*Quadrula aurea* and *Quadrula petrina*) were chosen for isotope analysis. Subsamples of shell carbonate powder were extracted sequentially in a transect from the hinge (oldest accreted material) towards the edge (newest accreted material) traversing growth increments in order to acquire individual isotope life histories for each shell. A computer-controlled micromill (ESI®) with an x-y-z moveable stage connected to a high-resolution camera system was used to pinpoint locations for subsample extraction along specified transects. Square rasters of 650 µm x 650 µm and a drilling depth of 100 µm were drilled for each subsample to extract a target powdered sample mass of 200 µg. This sample mass to meet the optimal mass requirements by the mass spectrometer that yields reliable isotope ratio measurements. A total of 166 subsamples were measured, ranging from 6 to 22 subsamples per shell depending on shell size. Average subsample mass was 184.5 ± 35.3 µg (1 standard deviation).

Subsamples were all extracted from the prismatic layer below the periostracum (organic outer layer of the shell) and above the nacreous layer. When the prismatic layer narrowed towards the growing edge of each shell, raster sizes were modified to fit within the prismatic layer but still yield minimum required masses for analyses. Once micromilling was completed, distances from the shell hinge to the centerpoint of each raster were measured using a microscope. Distances from the hinge to identified annual increments were also measurement to identify relationships between isotope values and increment deposition.

The carbon and oxygen-isotope measurements were made at the Core Facilities Laboratory at the University of Texas Marine Science Institute in Port Aransas, Texas. The method employed obtains simultaneous measurements of $\delta^{13}\text{C}$ and $\delta^{18}\text{O}$ values for each subsample. Briefly, the isotopic compositions were obtained by placing each subsample of powdered shell carbonate into an exetainer and sealing the contents with rubber septa. The vials were subsequently flushed with Helium for 5 minutes to remove atmospheric air. Phosphoric acid (H_3PO_4) was injected into the vials and allowed to equilibrate for 60 minutes at 70°C. Headspace CO_2 was analyzed for carbon and oxygen-isotope compositions using a Gasbench II device (Thermo Fisher Scientific) coupled

to a Thermo Fisher Scientific Delta V stable-isotope-ratio mass spectrometer. Isotope ratios are reported in standard delta notation where

$$\delta = \left[\left(\frac{R_{\text{sample}}}{R_{\text{standard}}} \right) - 1 \right] * 1000$$

And where R_{sample} and R_{standard} are the isotopic ratios (e.g. $^{18}\text{O}/^{16}\text{O}$ or $^{13}\text{C}/^{12}\text{C}$) of the sample and the standard, respectively, and values are in permil (‰) units. Delta values of both $\delta^{13}\text{C}$ and $\delta^{18}\text{O}$ in the mussel carbonate samples are reported relative to VPDB throughout this report. A two-point calibration of $\delta^{13}\text{C}$ to VPDB was achieved using repeated measurements of certified reference materials NBS-19 (+1.95‰) and LSVEC (−46.6‰). For measurements of NBS-19 throughout the analytical sessions, the average $\delta^{13}\text{C}$ was $+1.97 \pm 0.12\text{‰}$ (SD, $n=11$), and for LSVEC $-46.6 \pm 0.2\text{‰}$ (SD, $n=12$). International standards NBS-19 (−2.20‰) and NBS-18 (−23.2‰) were used to provide a two-point calibration curve for the oxygen-isotope compositions relative to VPDB. For NBS-19, the average $\delta^{18}\text{O}$ was $-2.24\text{‰} \pm 0.11\text{‰}$ (SD, $n=11$), and for NBS-18, $-23.1\text{‰} \pm 0.2\text{‰}$ (SD, $n=7$). Internal laboratory calcite standard Suprapur was used to evaluate the accuracy and precision of the carbon and oxygen isotope results: $-41.5 \pm 0.2\text{‰}$ (SD, $n=13$) and $-14.0 \pm 0.2\text{‰}$ (SD, $n=7$), which were well within the accepted range of -41.5‰ and -14.0‰ , respectively.

Once subsample isotope ratios were obtained and distances measured for subsamples and increments, values were plotted individually for each sampled shell to create lifetime transects of both $\delta^{13}\text{C}$ and $\delta^{18}\text{O}$ variability across increments. In addition, linear regressions comparing $\delta^{13}\text{C}$ and $\delta^{18}\text{O}$ values for all subsamples from an individual shell were calculated in order to assess whether ratios were positively, negatively or not related over the time series for each shell.

In order to compare isotope values with ambient environmental parameters, we first used identified increments to designate subsamples that fell within dated annual increments. All subsamples that fell within dated increments were averaged together to yield a combined annual isotope signature for $\delta^{13}\text{C}$ and $\delta^{18}\text{O}$ values. This was done because the number of subsamples within a given year varied by shell and calendar year due to age-related growth declines and differences in growth rates among individuals. Thus, subannual resolution of isotope values was inconsistent. An annually-resolved assessment was therefore the lowest temporal resolution possible. Samples were averaged across species and specimens to investigate overall patterns in annual isotope shifts recorded by multiple individuals within a geographic location.

Environmental data on air temperature and discharge were obtained for the same identified years for comparisons with isotope values. Hadley CRU 0.5° gridded average annual air temperature (°C) were extracted from the four closest grid cells to the study site and averaged for

comparison with mussel isotopic parameters. Monthly discharge measurements (cubic feet per second) for the Guadalupe River were retrieved from the USGS water monitoring station at Gonzales, TX (USGS Station ID 08173900). Monthly discharge and temperature measurements were averaged by year to obtain average monthly discharge for the years 2009-2014 corresponding to annual isotope measurements. The maximum and minimum monthly discharge for each year was also extracted for comparison to test whether isotope values were driven by extreme values in flow. Finally, the total range in monthly discharge per year was calculated as the maximum minus the minimum monthly discharge to determine if annual fluctuation in flow explained isotope variability. Linear regressions between isotope values (both $\delta^{13}\text{C}$ and $\delta^{18}\text{O}$) and average monthly air temperature, average monthly discharge, maximum monthly discharge, minimum monthly discharge, and range in monthly discharge were calculated and assessed for statistically significant departure from a slope of zero.

Results and Discussion

Growth-increment widths

All twenty-two *Q. petrina* and ten *Q. aurea* that had been collected were thin-sectioned and visually evaluated for the presence of growth increments. For both species growth increments were indistinct and difficult to identify, though they were somewhat more clearly delineated in *Q. petrina* relative to *Q. aurea* (Figure 1, 2). A major criterion for discerning a true increment was whether it was continuous through the nacreous and prismatic layers, as has been widely applied for other mussel species (Black et al. 2010). There were, however, many apparent “false” increments that appeared to be cracks in the shell material, which may have been formed in response to mechanical damage as could occur during a flooding event. Cracks were generally very narrow with high contrast to the rest of the shell and often occurred near true increment boundaries. These false-ring “cracks” are common in other species of mussels and complicate efforts to crossdate (Black et al. 2010). Overall, increments tended to be more diffuse and relatively difficult to identify in the earliest years of growth (Figure 1, 2).



Figure 1. Thin sections of the oldest *Quadrula aurea*, which were used in isotope analysis. Red arrows indicate the best estimates of growth-increment boundaries. Notice the wells drilled in the prismatic layer to sample carbonate material for isotope analysis. Isotope values are available for those wells with yellow numbers. Sample numbers are *Q. aurea* 1, 4, and 5 from top to bottom image.

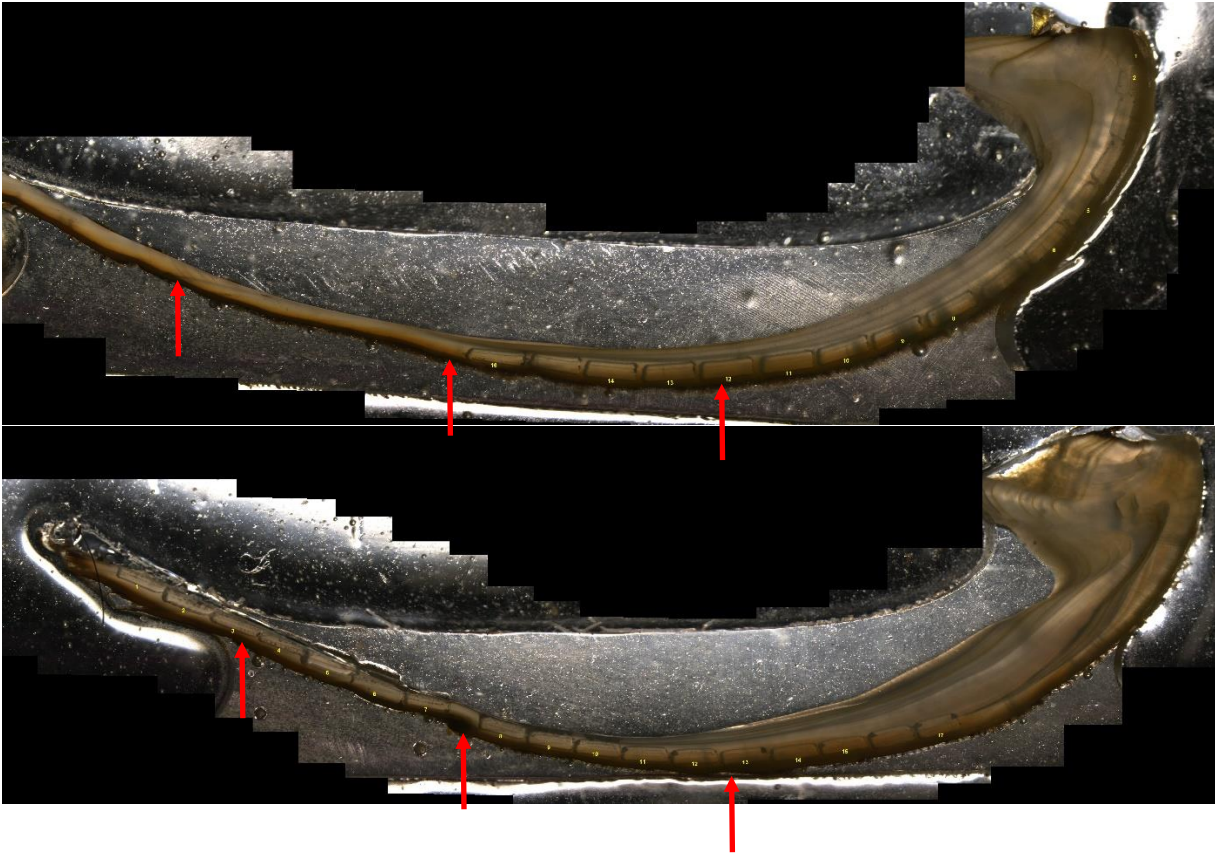
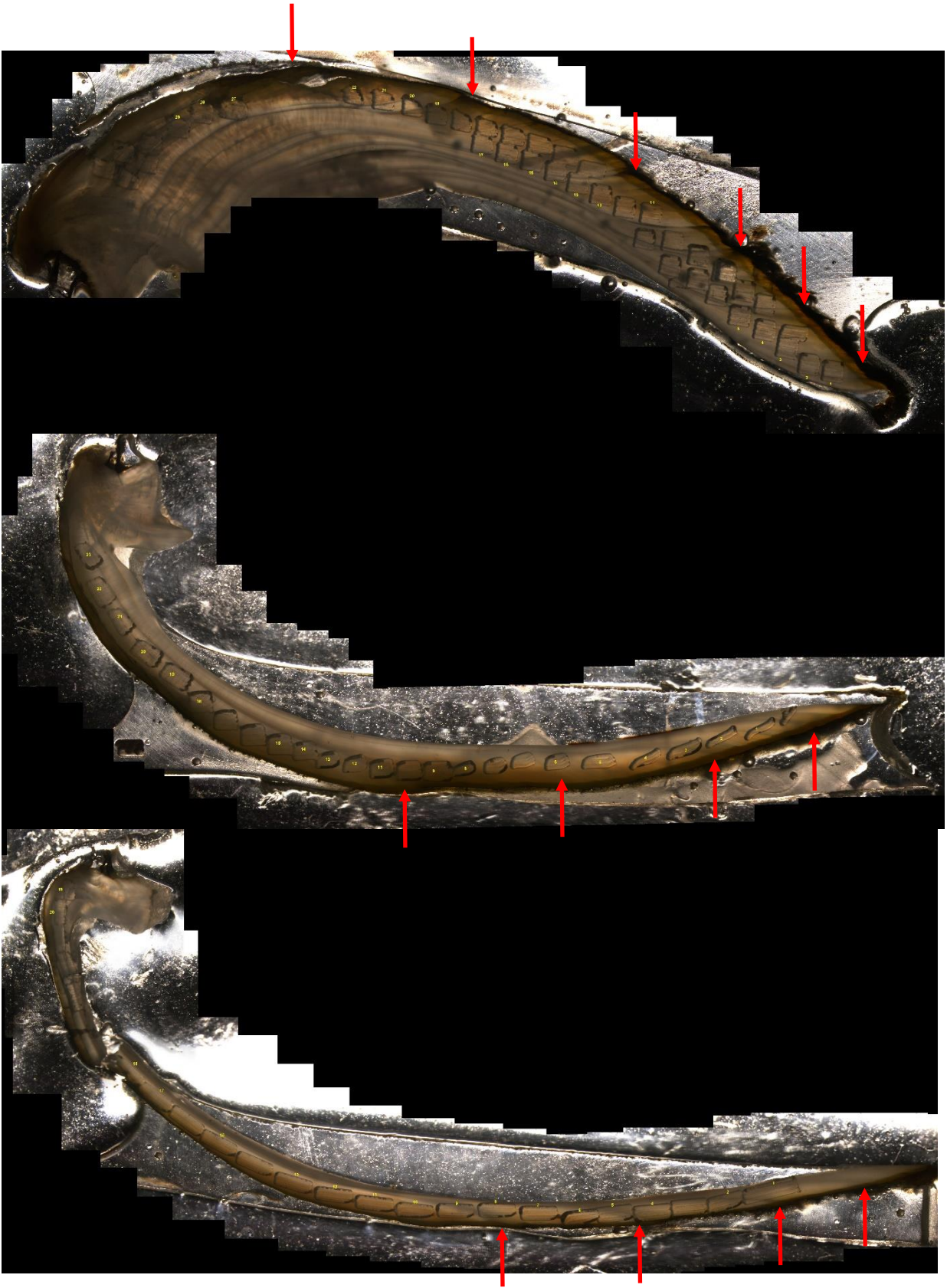


Figure 1 (continued). Thin sections of the oldest *Quadrula aurea*, which were used in isotope analysis. Red arrows indicate the best estimates of growth-increment boundaries. Notice the wells drilled in the prismatic layer to sample carbonate material for isotope analysis. Isotope values are available for those wells with yellow numbers. Sample numbers are *Q. aurea* 6 and 7 from top to bottom image.



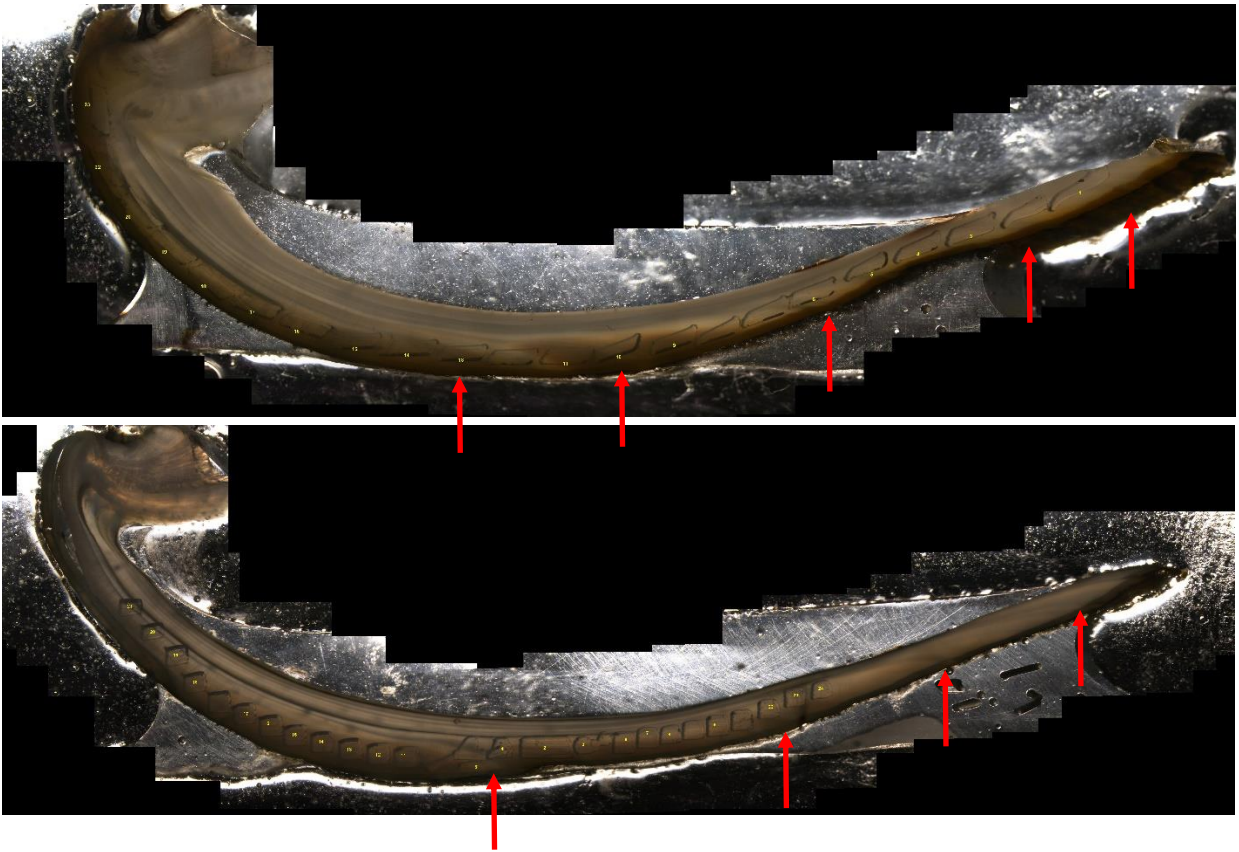


Figure 2 (including previous page). Thin sections of the oldest *Quadrula petrina*, which were used in isotope analysis. Red arrows indicate the best estimates of growth-increment boundaries. Notice the wells drilled in the prismatic layer to sample carbonate material for isotope analysis. Isotope values are available for those wells with yellow numbers. Sample numbers are *Q. petrina* 9, 15, 19, 21, and 22 from top to bottom image.

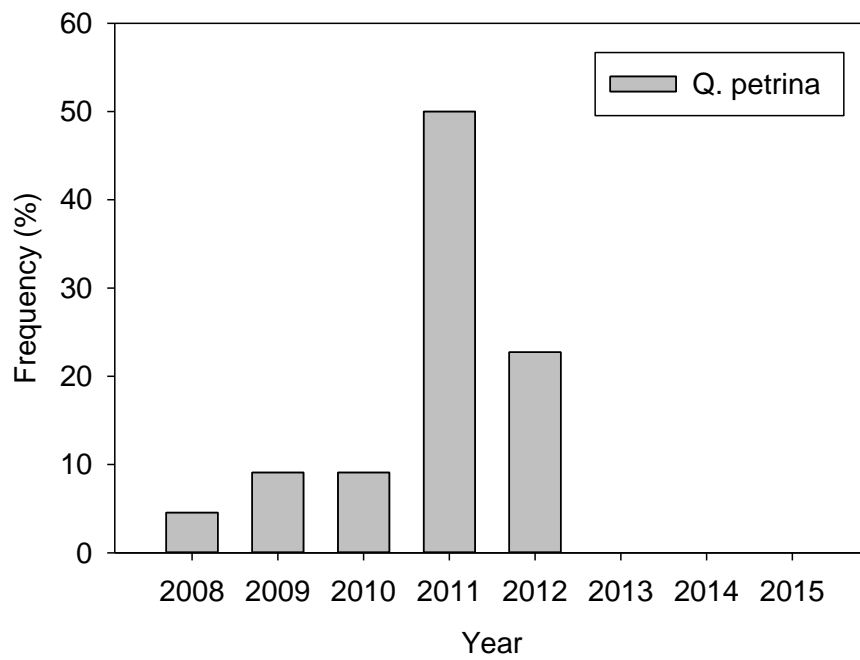
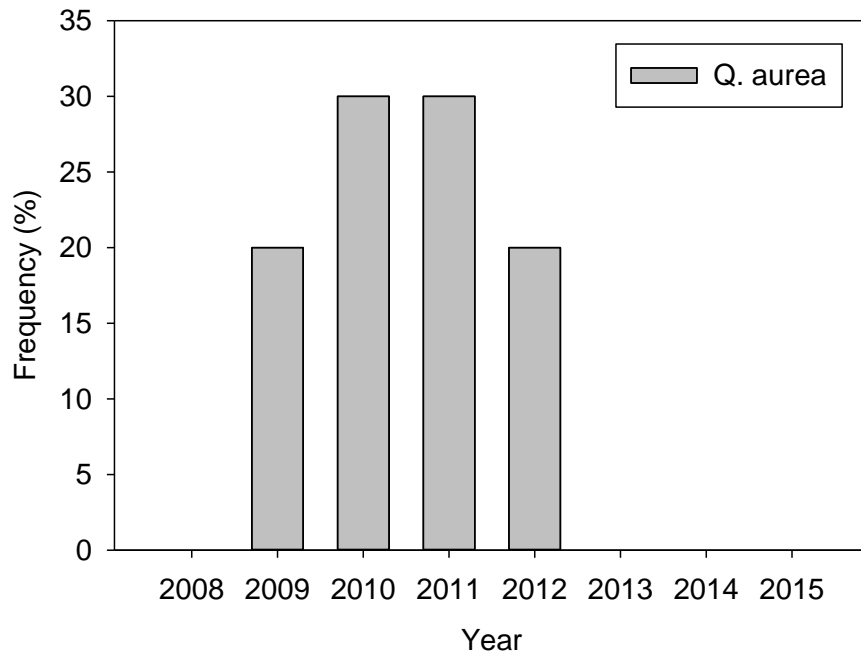


Figure 3. Frequency histogram of freshwater mussel establishment dates.

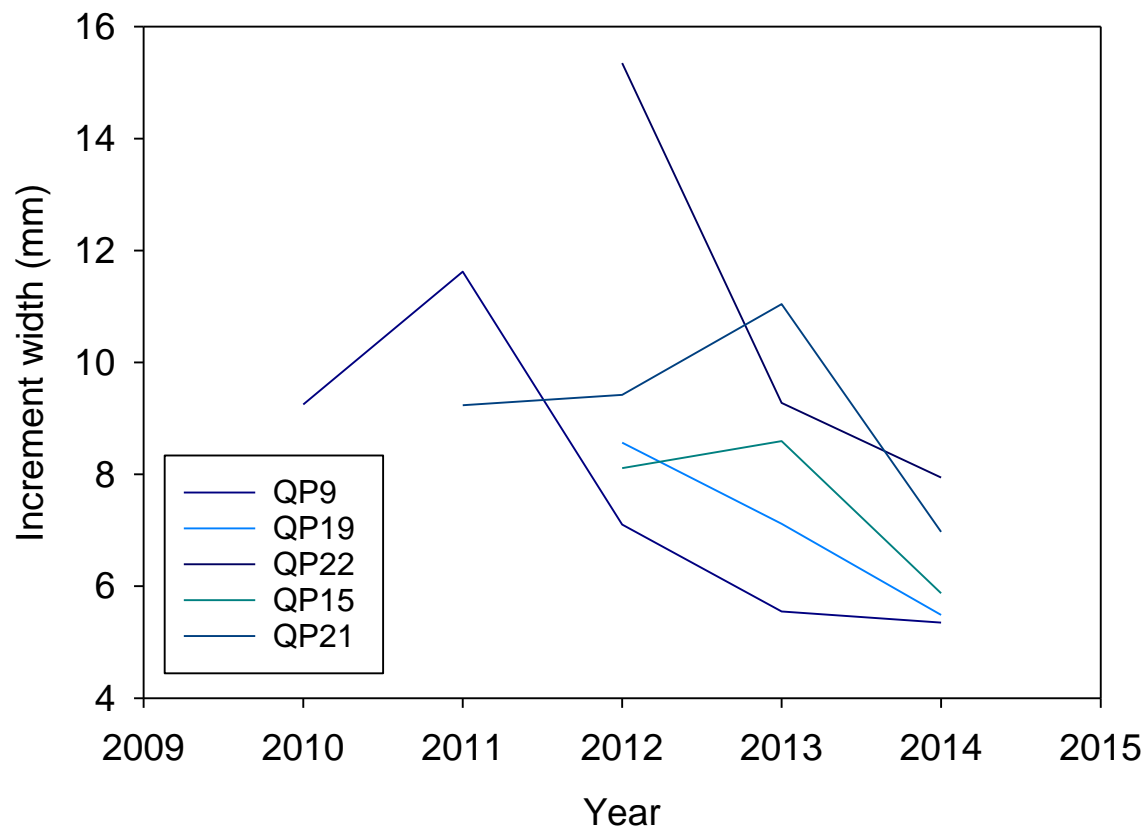


Figure 4. Growth-increment widths from the five oldest *Q. petrina* samples.

Visual analysis of growth increments in these samples suggest they are all quite young in age, all establishing after 2007 (Figure 3). Indeed, the vast majority were less than five years in age, especially the *Q. aurea* samples (Figure 3). *Q. petrina* did appear to have episodic recruitment with a large pulse in 2011 to which half the sample dates (Figure 3), which may suggest some environmental control on reproduction in this species. Give these short lifespans, crossdating was not possible. There was not sufficient overlap by which to cross-match growth “barcodes” with and degree of confidence. Although crossdating has been possible in relatively short-lived species such as flatfish in the Bering Sea (Matta et al. 2010), interannual variability was quite strong and consistent and fish lived at least ten years, and in some cases, more than thirty. In the present study, mussels were much younger, and to the extent that many had only one or two complete increments that could be measured. Even when the oldest *Q. petrina* samples are measured, there is not clear synchrony in interannual growth patterns among individuals (Figure 4). Although

crossdating and chronology development have been possible for freshwater mussels elsewhere in the Southeast (Rypel et al. 2008, 2009) and in the Pacific Northwest (Black et al. 2010, Black et al. 2015), these mussels from Texas do not meet the minimum requirements. Growth-increments do appear to be sufficiently well delineated in older individuals, so this may be possible with a sample set of older animals. Nonetheless, the present sample set does suggest that these mussels appear to form annual increments, are short-lived, and may have episodic recruitment.

Isotopic analysis: individual transects

The five oldest *Q. aurea* and *Q. petrina* were sampled for isotopes. Lifetime transects of isotope ratios were highly variable among shell samples in both sampled species. The time period covered by transects varied according to identified increments. Tight spacing of some increments meant that multiple subsamples within annual increments were not consistently obtained, and thus assessment of subseasonal variation in isotopes that might be expected due to seasonal temperature or productivity fluctuations was not consistently possible. This inconsistency meant that the temporal resolution of a given subsample varied from approximately one-three months to annual. The initial goal of using isotopes to assist in resolving placement of annual increments (and identifying seasonal climate patterns to help identify missing annuli) was therefore not met.

Table 1. Values of $\delta^{13}\text{C}$ (‰) from subsamples within confidently identified annual increments in mussel shells. Values are provided for one shell from *Quadrula aurea* (QA) and five shells from *Quadrula petrina* (QP). Shell sample numbers are indicated in the first row.

	QA07	QP09	QP15	QP19	QP21	QP22	Average
2009	-	-	-	-	-8.4	-	-8.4
2010	-	-	-	-7.4	-8.1	-	-7.8
2011	-9.1	-	-8.1	-8.6	-8.8	-6.7	-8.2
2012	-8.3	-7.3	-9.2	-7.7	-8.9	-8.8	-8.3
2013	-8.0	-6.6	-8.7	-7.3	-9.1	-9.1	-8.1
2014	-7.7	-	-	-	-	-	-7.7

Table 2. Values of $\delta^{18}\text{O}$ (‰) from subsamples within confidently identified annual increments in mussel shells. Values are provided for one shell from *Quadrula aurea* (QA) and five shells from *Quadrula petrina* (QP). Shell sample numbers are indicated in the first row.

	QA07	QP09	QP15	QP19	QP21	QP22	Average
2009	-	-	-	-	-3.6	-	-3.6
2010	-	-	-	-3.8	-3.8	-	-3.8
2011	-4.6	-	-5.1	-4.7	-3.8	-3.8	-4.4
2012	-4.0	-4.0	-4.1	-3.5	-3.5	-4.9	-4.0
2013	-3.2	-3.5	-3.8	-3.7	-3.7	-4.7	-3.8
2014	-3.8	-	-	-	-	-	-3.8

Regressions of $\delta^{18}\text{O}$ values against $\delta^{13}\text{C}$ values yielded highly variable relationships among individuals (Figures 4-24). Slopes were positive for seven of the individuals (three of *Q. aurea* and four of *Q. petrina*), negative for two individuals (one of *Q. aurea* and one of *Q. petrina*) and flat for the remaining *Q. aurea* individual. Scatter in these relationships was also individually variable, with R^2 values ranging from as low as 0.004 (*Q. aurea* Sample #01) and as high as 0.81 (*Q. aurea* Sample #05). Patterns for some individuals indicated strongly coincident shifts in both isotope ratios, such as *Q. aurea* Sample #05 (Figure 9.) which recorded a dip in both isotope ratios close to the hinge and a dramatic spike in both isotope ratios towards the end of the transect. This consistent simultaneous shift in the same direction led to a strong positive relationship for this individual. However, other individuals showed evidence of both positive and negative relationships within the same transect. For instance, *Q. petrina* Sample #09 showed negative relationships between isotopes towards the beginning of the transect but positive relationships towards the end, resulting in a high degree of scatter in the overall relationship over its lifetime (Figure 16). This inconsistency meant that either positive or negative shifts at a subannual resolution could not be used to indicate age for shells with ambiguous increments. This result is likely driven in part by the inconsistent ability to extract subannual samples for isotope measurements due to inconsistent growth patterns between individuals. Future assessments of isotope variability in these shells will likely require high spatial resolution of isotope mapping, such as ion microprobe methods that avoid the need for micromilling and extraction of significant amounts of powdered samples.

Relationships between environmental parameters and annually averaged isotope ratios were more informative (Figures 26-29). Regressions between $\delta^{18}\text{O}$ and $\delta^{13}\text{C}$ values and average monthly air temperature were both negative, with increasing temperature associated with lower isotope ratios values. This was expected for $\delta^{18}\text{O}$ given the commonly observed decrease in values with increasing temperature in many shell-forming organisms including bivalves due to temperature-induced fractionation during precipitation of carbonate (Sharp 2007, Wingard and Surge 2017). Despite this expected relationship, there was scatter in the regression, particularly in 2009 and 2011 when isotope ratios were higher and lower than expected, respectively (Figure 25). Because of this, the regression was not statistically significant ($P = 0.20$). The regression between $\delta^{13}\text{C}$ values and temperature was also negative, and was the only regression that was found to be statistically significantly different than a slope of zero ($P = 0.04$). The interpretation of relationship was less clear. Carbon isotopes in bivalve shells is a result of complex interactions between external factors affecting isotopic composition of the DIC taken up for shell precipitation and internal metabolic processes that alter carbon isotopic values of the internal DIC pool prior to precipitation (McConnaughey and Gillikin 2008). In addition, the relative contribution of respired metabolic carbon versus ambient DIC to the carbon used to precipitate shells can vary between and within species (Gillikin et al. 2007, Wanamaker et al. 2007, Gillikin et al. 2009, Poulain et al. 2010). The strong relationship with annual temperature and shell carbon isotopes might therefore be a result of shifts in net ecosystem metabolism that alters the composition of ambient DIC in river water, differential growth performance and metabolic rates driven by temperature, or both (Walther and Rowley 2013). Although shell carbon isotopes appear to be diagnostic of annual climate conditions in these two mussel species, the mechanism driving this relationship is currently ambiguous.

Relationships between isotopes and average, maximum, minimum and range of monthly were all weakly positive and not statistically significant (Figures 26-29). River flow dynamics, at least on an annual basis, thus do not appear to be faithfully recorded by isotope markers in these two species.

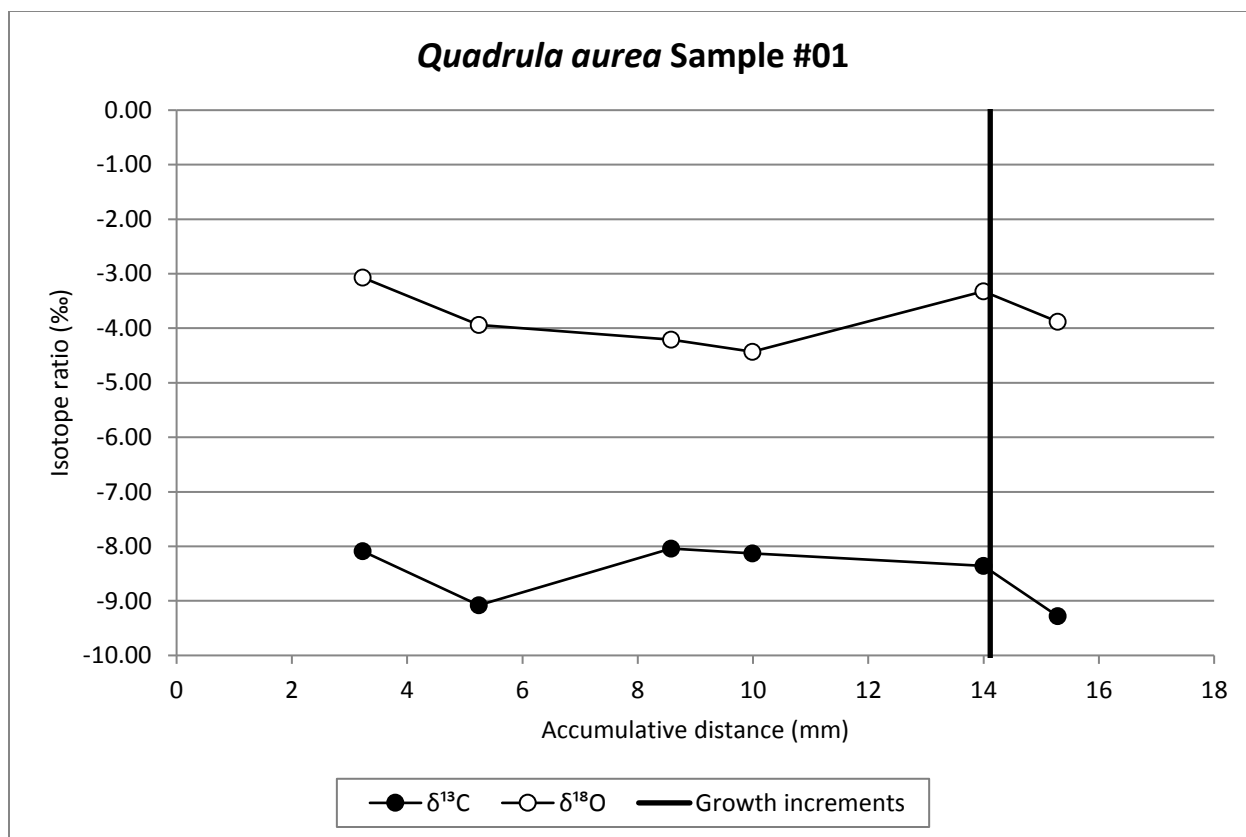


Figure 5. Isotope ratios across shell increments in *Quadrula aurea* sample #01. Distances measured outward from hinge. Isotope ratios reported in standard ‰ notation.

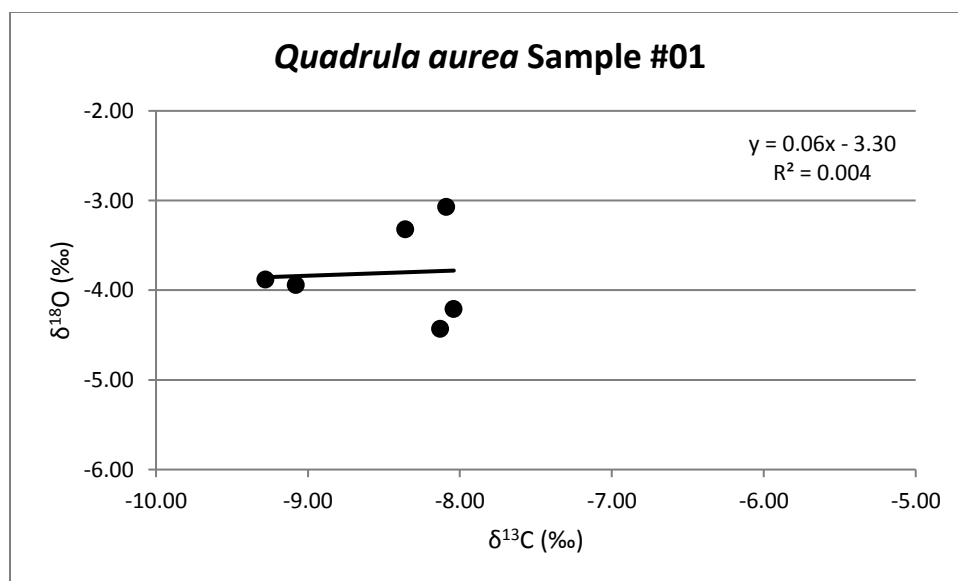


Figure 6. Relationship between $\delta^{13}\text{C}$ and $\delta^{18}\text{O}$ isotope ratios from *Quadrula aurea* sample #01.

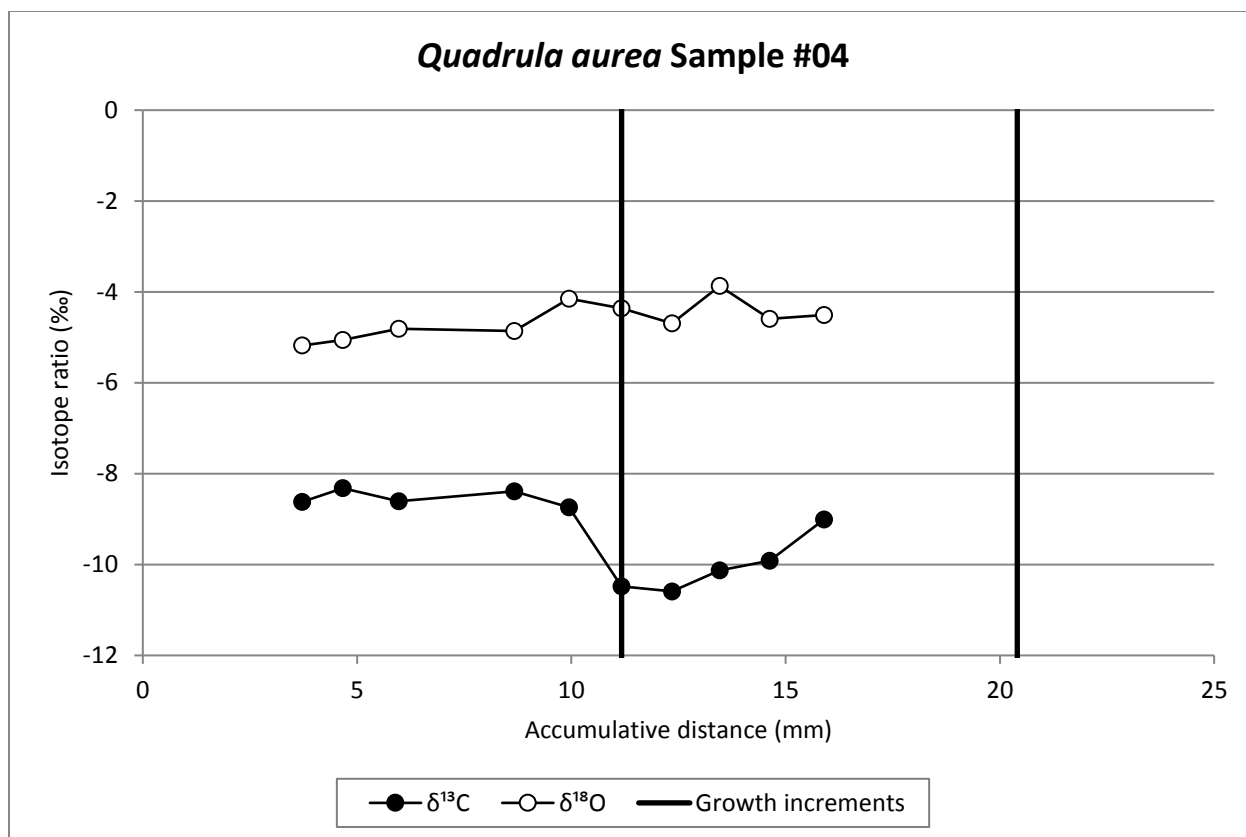


Figure 7. Isotope ratios across shell increments in *Quadrula aurea* sample #04. Distances measured outward from hinge. Isotope ratios reported in standard ‰ notation.

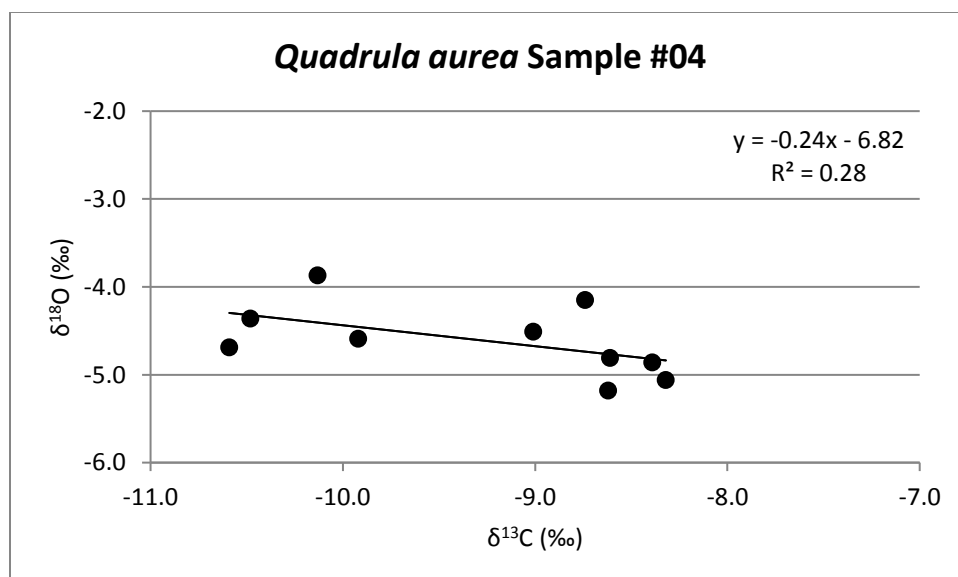


Figure 8. Relationship between $\delta^{13}\text{C}$ and $\delta^{18}\text{O}$ isotope ratios from *Quadrula aurea* sample #04.

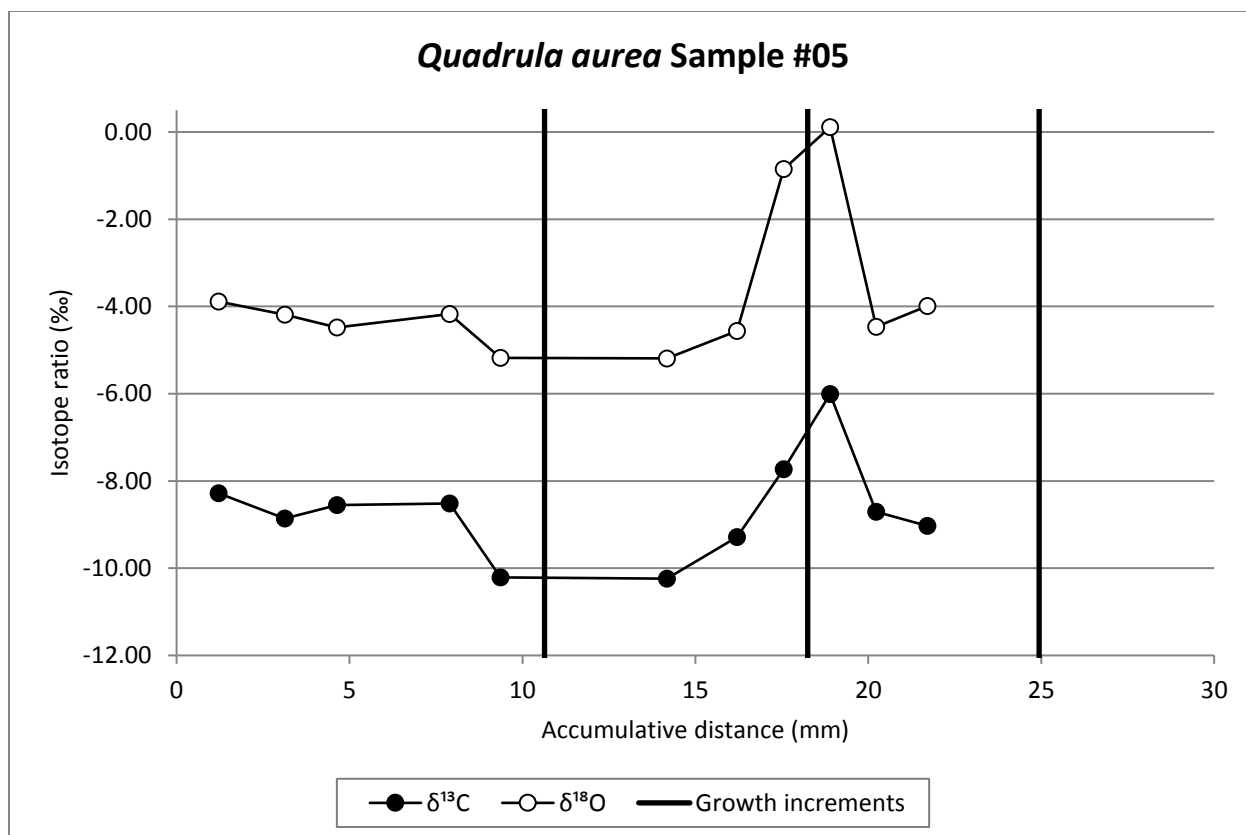


Figure 9. Isotope ratios across shell increments in *Quadrula aurea* sample #05. Distances measured outward from hinge. Isotope ratios reported in standard ‰ notation.

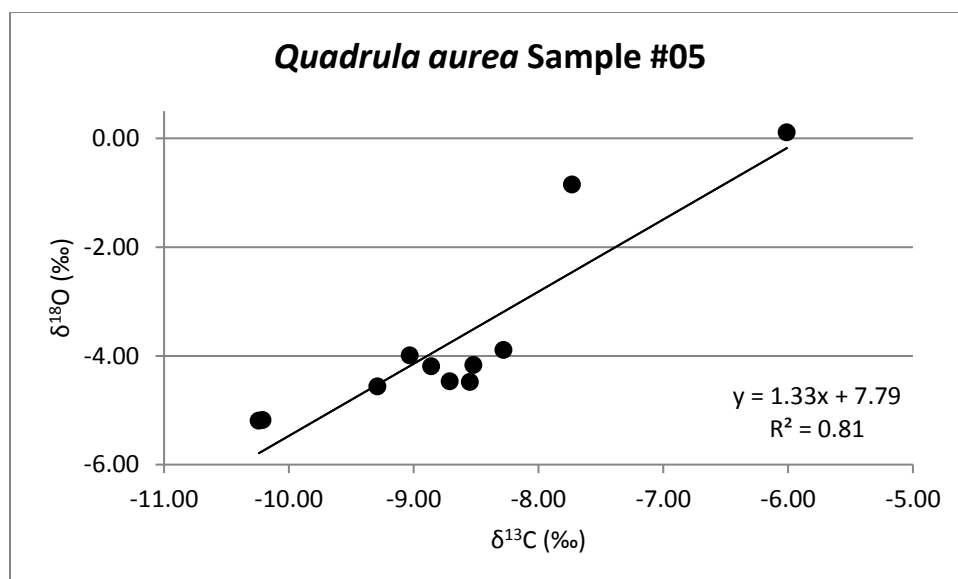


Figure 10. Relationship between $\delta^{13}\text{C}$ and $\delta^{18}\text{O}$ isotope ratios from *Quadrula aurea* sample #05.

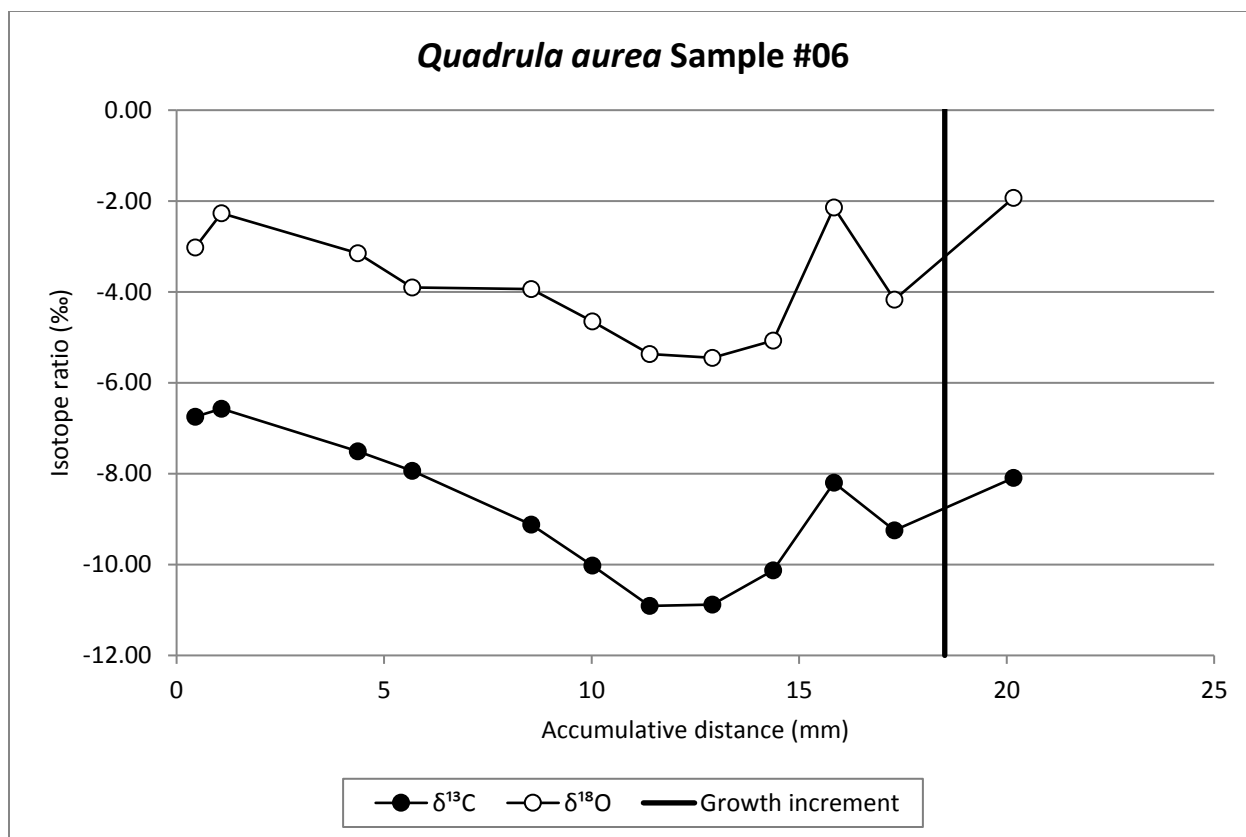


Figure 11. Isotope ratios across shell increments in *Quadrula aurea* sample #06. Distances measured outward from hinge. Isotope ratios reported in standard ‰ notation.

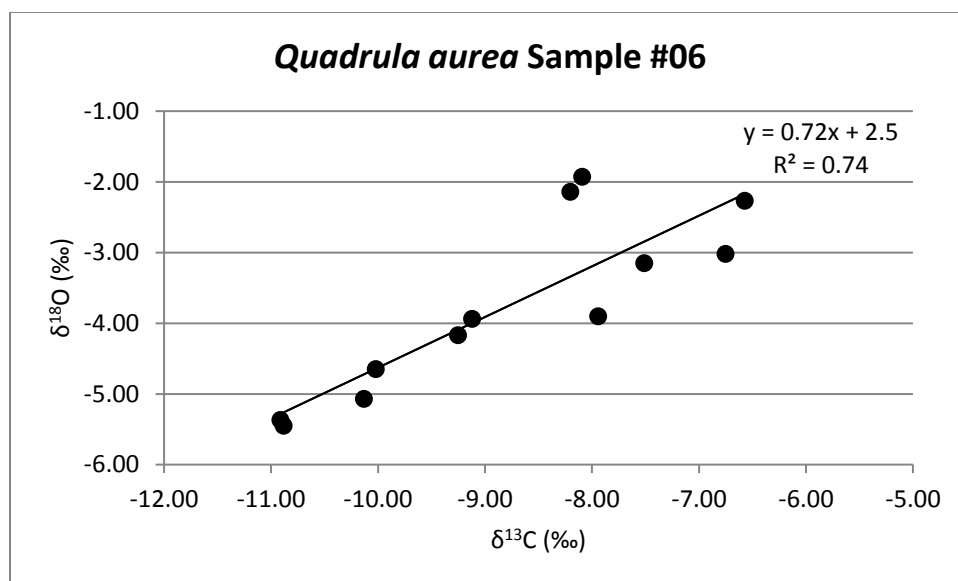


Figure 12. Relationship between $\delta^{13}\text{C}$ and $\delta^{18}\text{O}$ isotope ratios from *Quadrula aurea* sample #06.

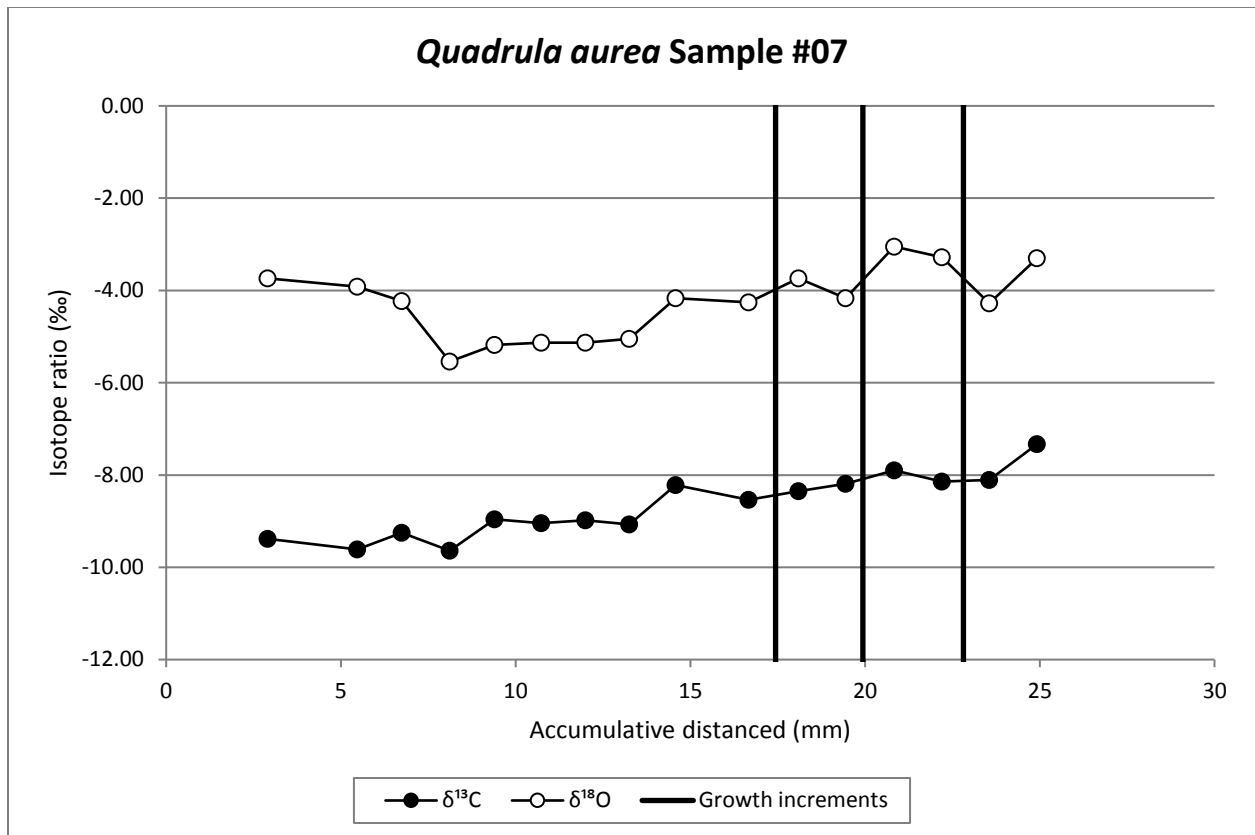


Figure 13. Isotope ratios across shell increments in *Quadrula aurea* sample #07. Distances measured outward from hinge. Isotope ratios reported in standard ‰ notation.

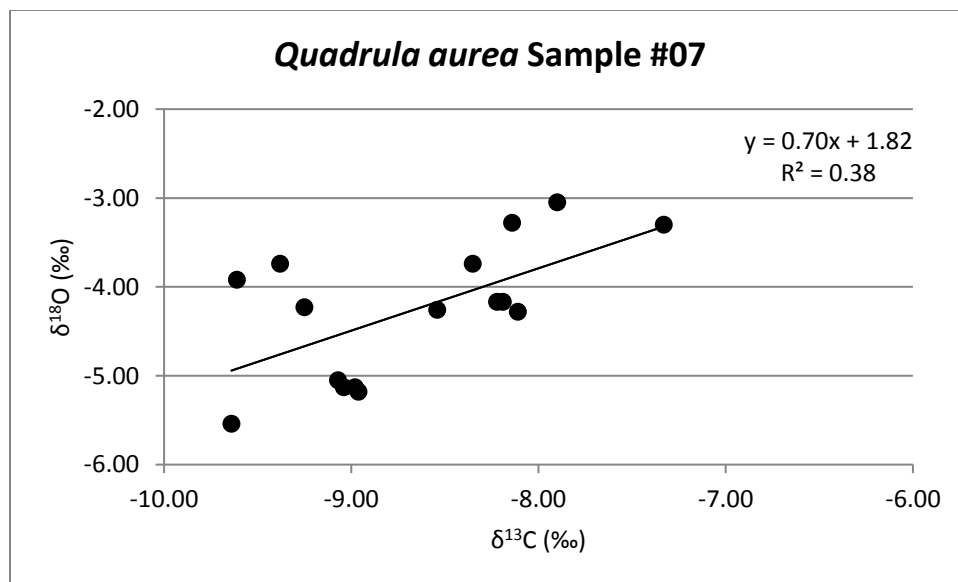


Figure 14. Relationship between $\delta^{13}\text{C}$ and $\delta^{18}\text{O}$ isotope ratios from *Quadrula aurea* sample #07.

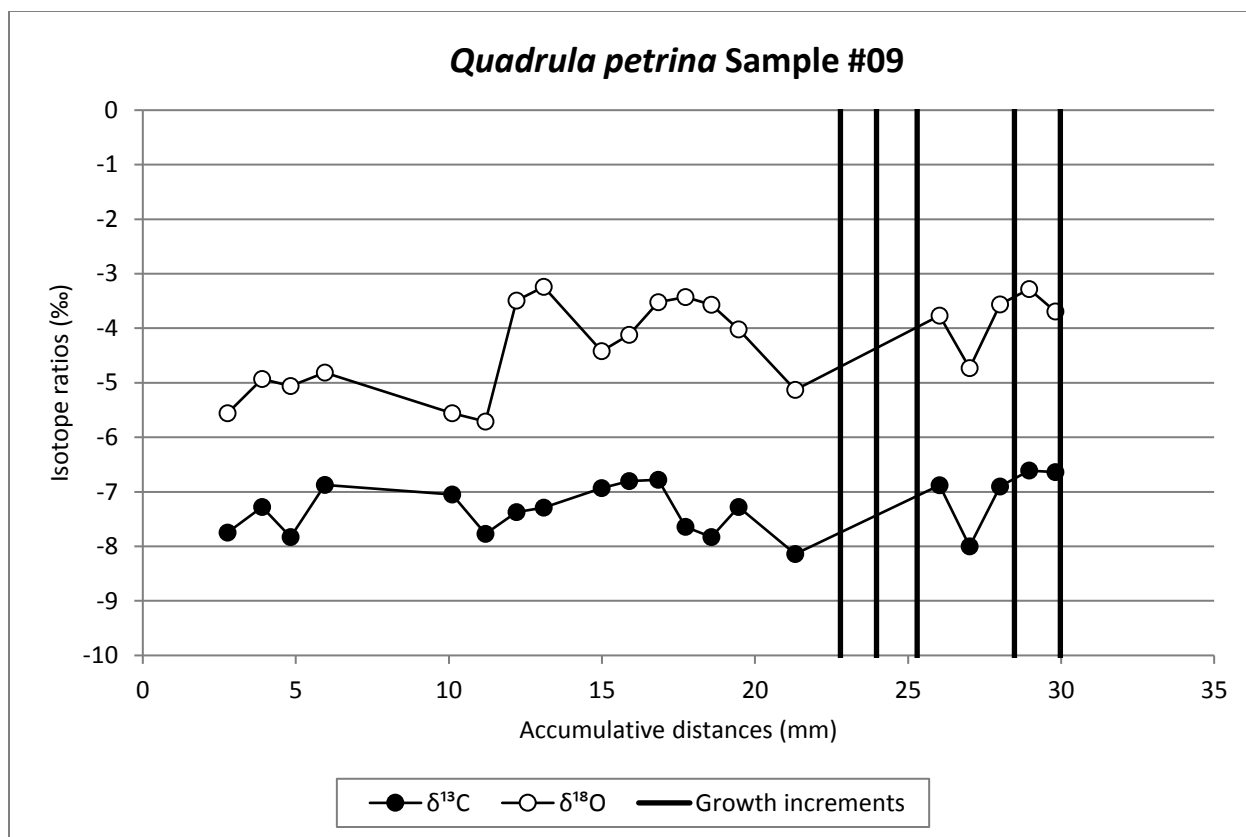


Figure 15. Isotope ratios across shell increments in *Quadrula petrina* sample #09. Distances measured outward from hinge. Isotope ratios reported in standard ‰ notation.

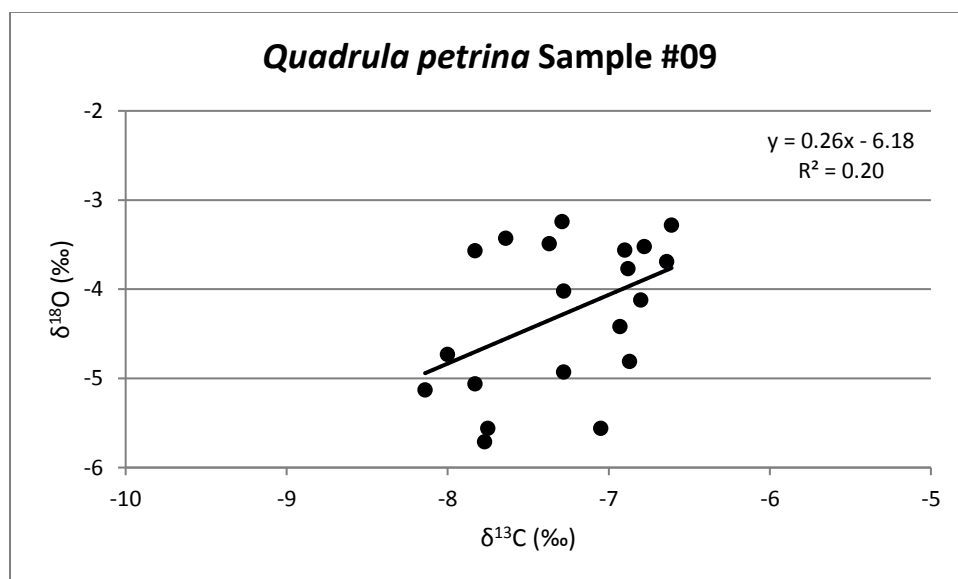


Figure 16. Relationship between $\delta^{13}\text{C}$ and $\delta^{18}\text{O}$ isotope ratios from *Quadrula petrina* sample #09.

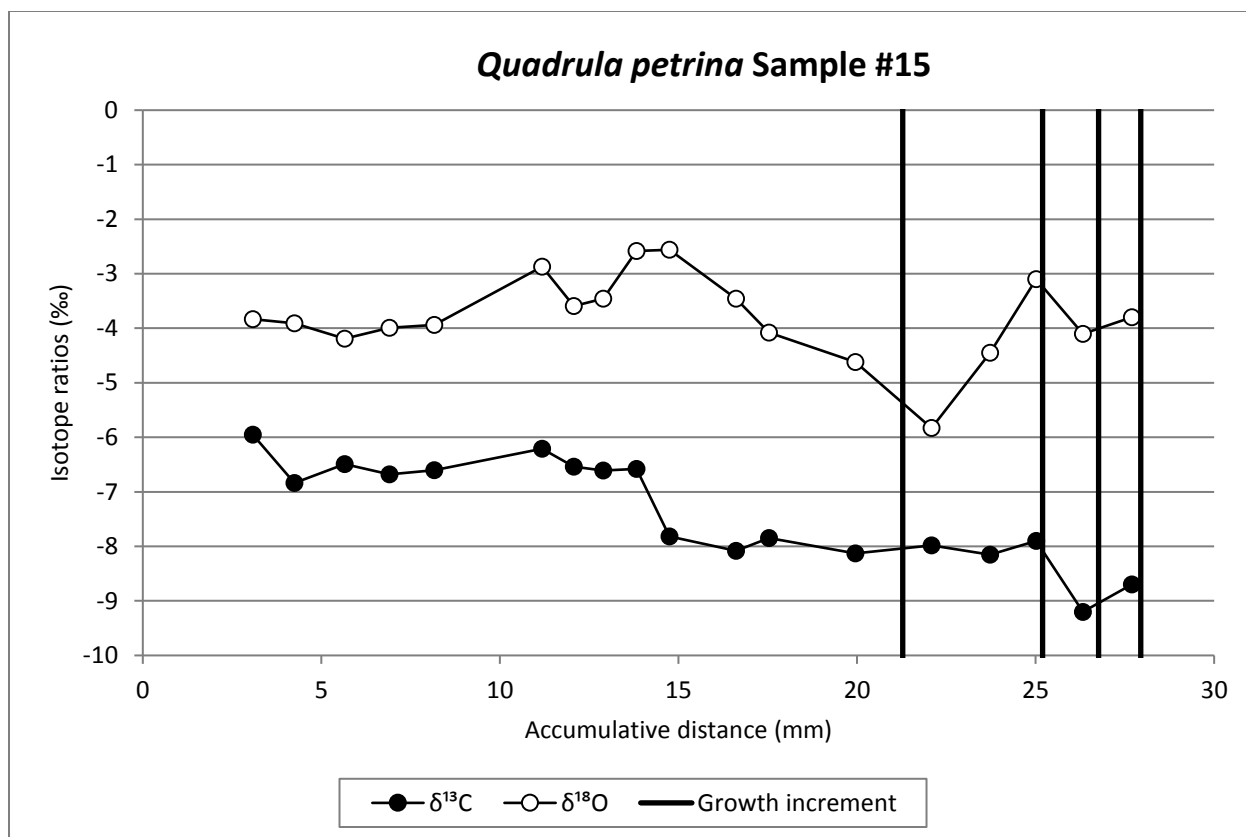


Figure 17. Isotope ratios across shell increments in *Quadrula petrina* sample #15. Distances measured outward from hinge. Isotope ratios reported in standard ‰ notation.

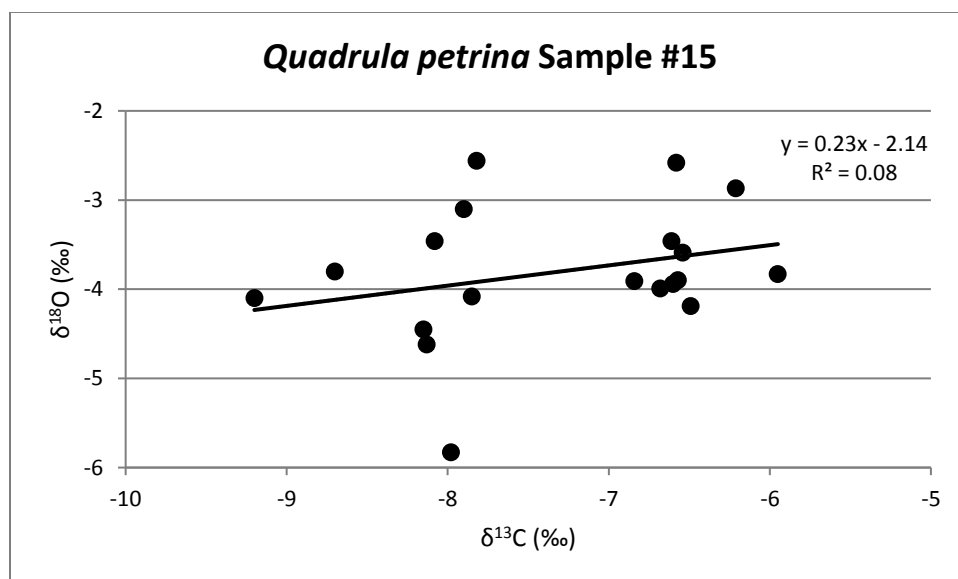


Figure 18. Relationship between $\delta^{13}\text{C}$ and $\delta^{18}\text{O}$ isotope ratios from *Quadrula petrina* sample #15.

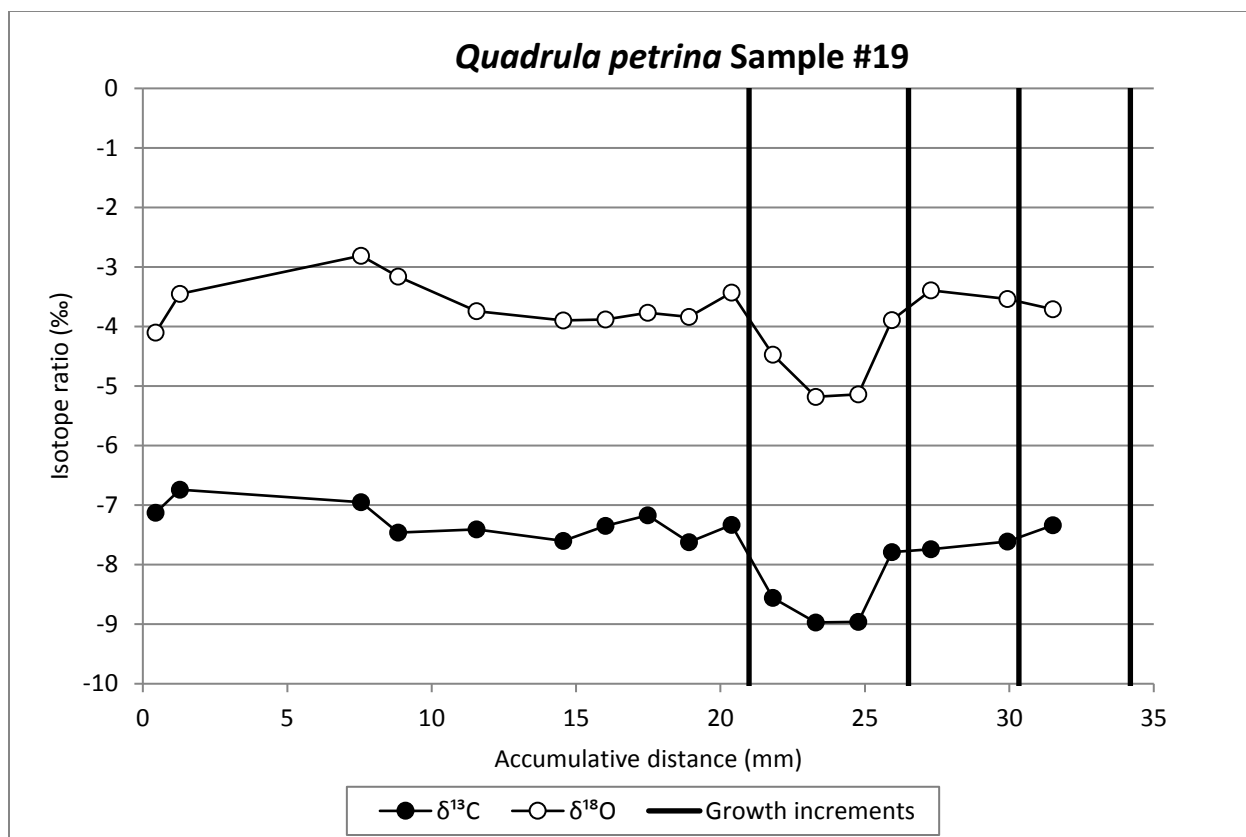


Figure 19. Isotope ratios across shell increments in *Quadrula petrina* sample #19. Distances measured outward from hinge. Isotope ratios reported in standard ‰ notation.

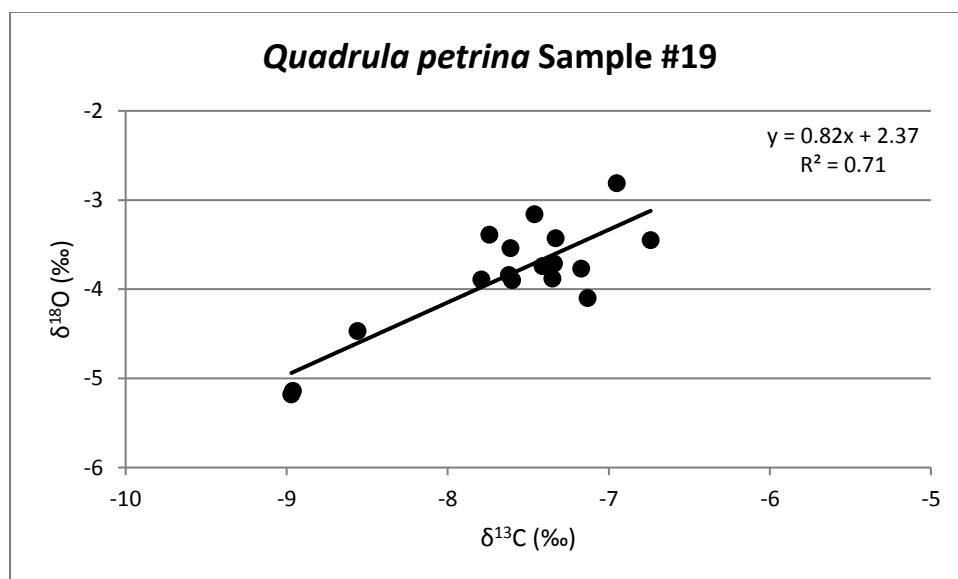


Figure 20. Relationship between $\delta^{13}\text{C}$ and $\delta^{18}\text{O}$ isotope ratios from *Quadrula petrina* sample #19.

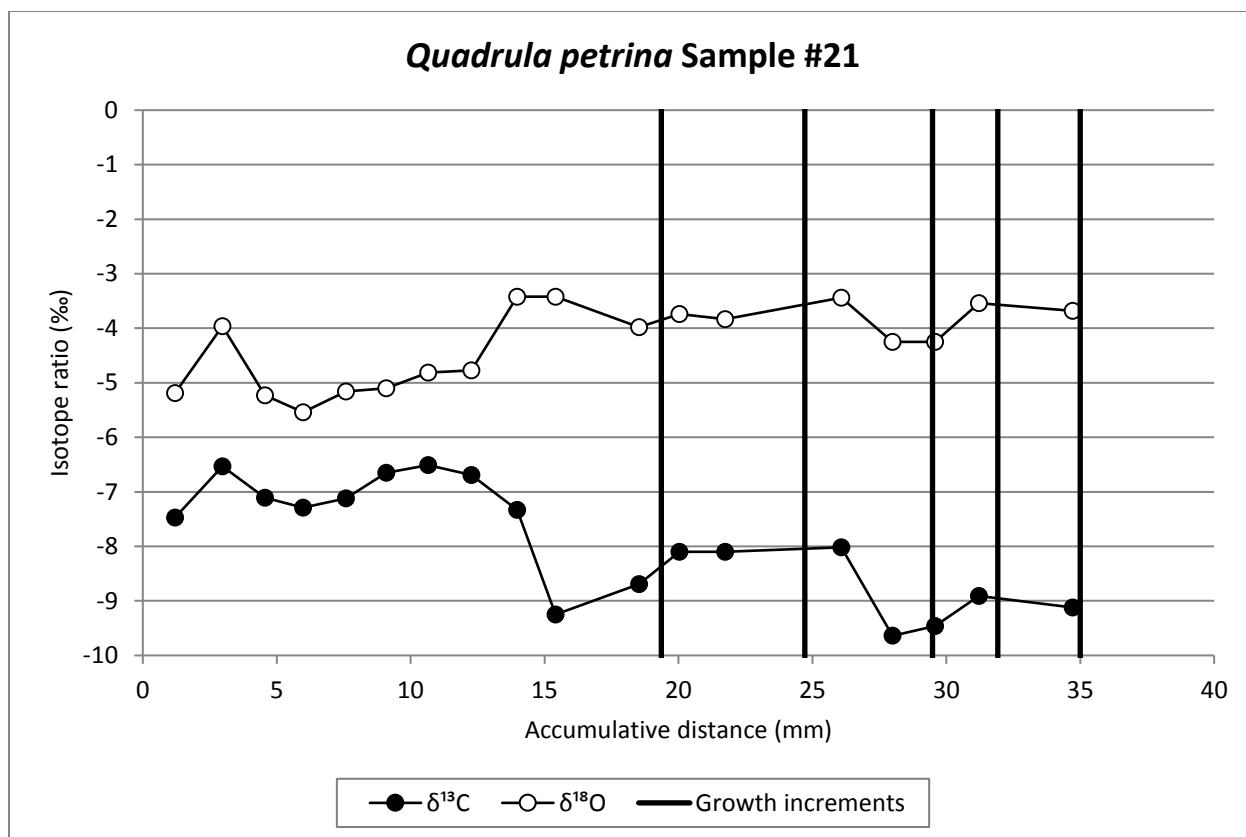


Figure 21. Isotope ratios across shell increments in *Quadrula petrina* sample #21. Distances measured outward from hinge. Isotope ratios reported in standard ‰ notation.

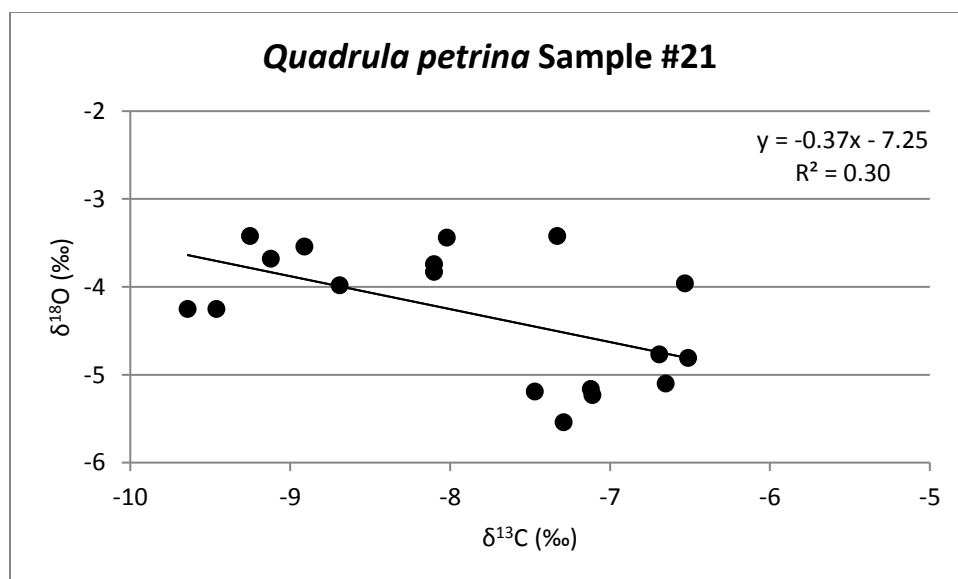


Figure 22. Relationship between $\delta^{13}\text{C}$ and $\delta^{18}\text{O}$ isotope ratios from *Quadrula petrina* sample #21.

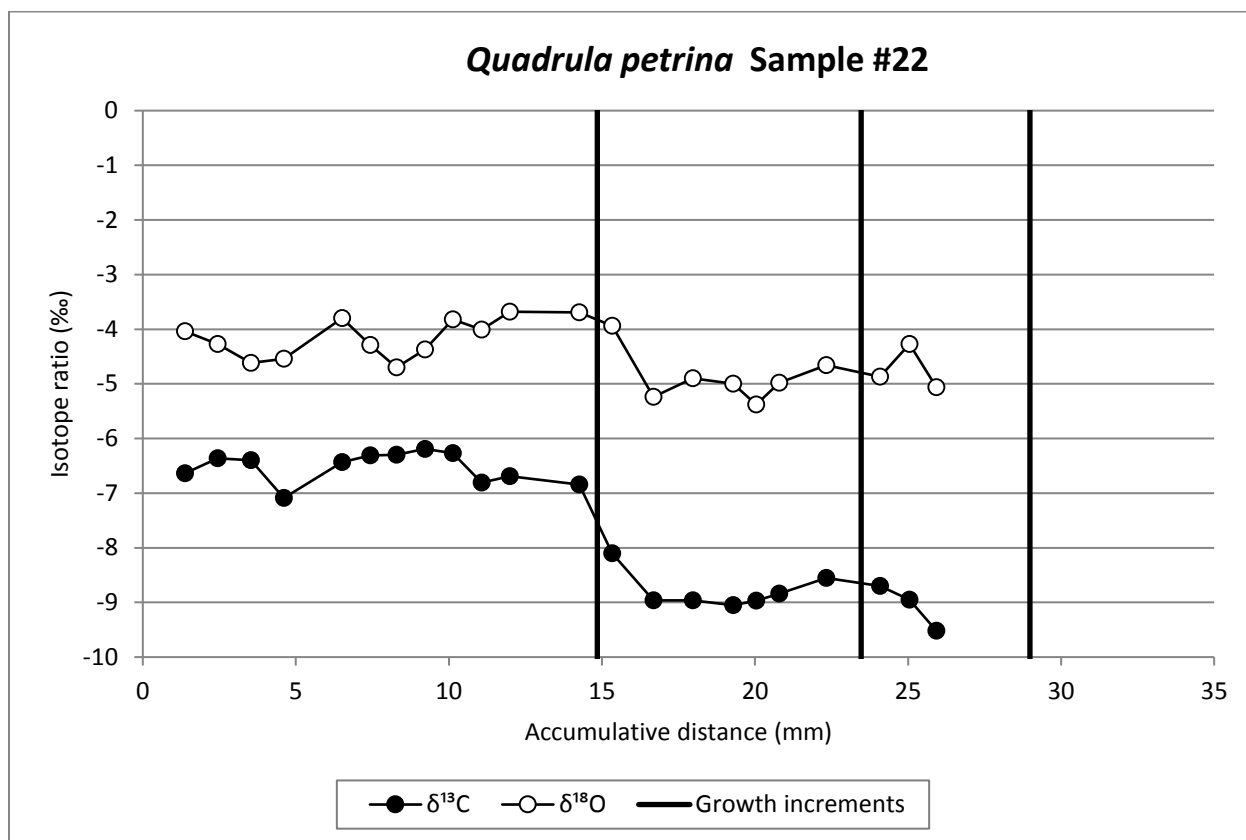


Figure 23. Isotope ratios across shell increments in *Quadrula petrina* sample #22. Distances measured outward from hinge. Isotope ratios reported in standard ‰ notation.

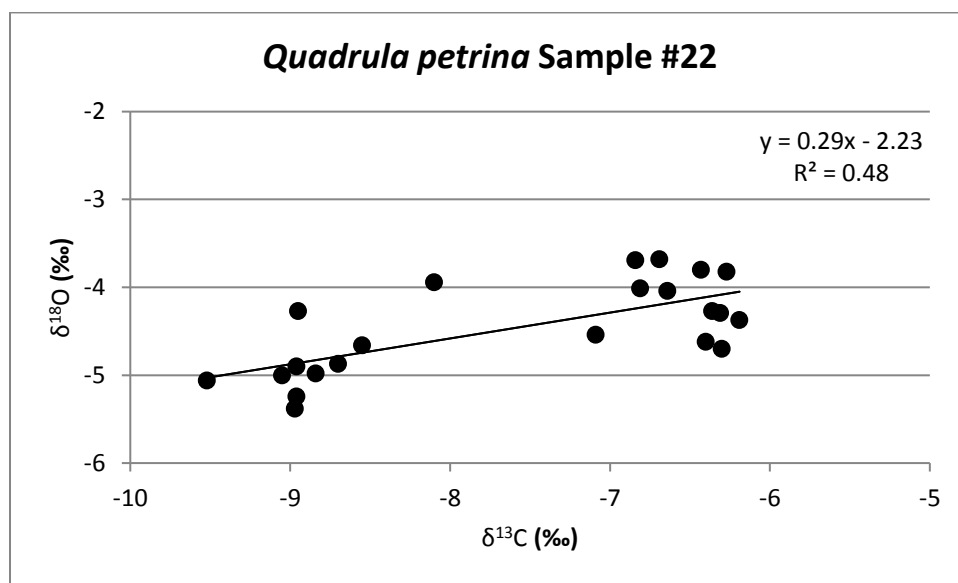


Figure 24. Relationship between $\delta^{13}\text{C}$ and $\delta^{18}\text{O}$ isotope ratios from *Quadrula petrina* sample #22.

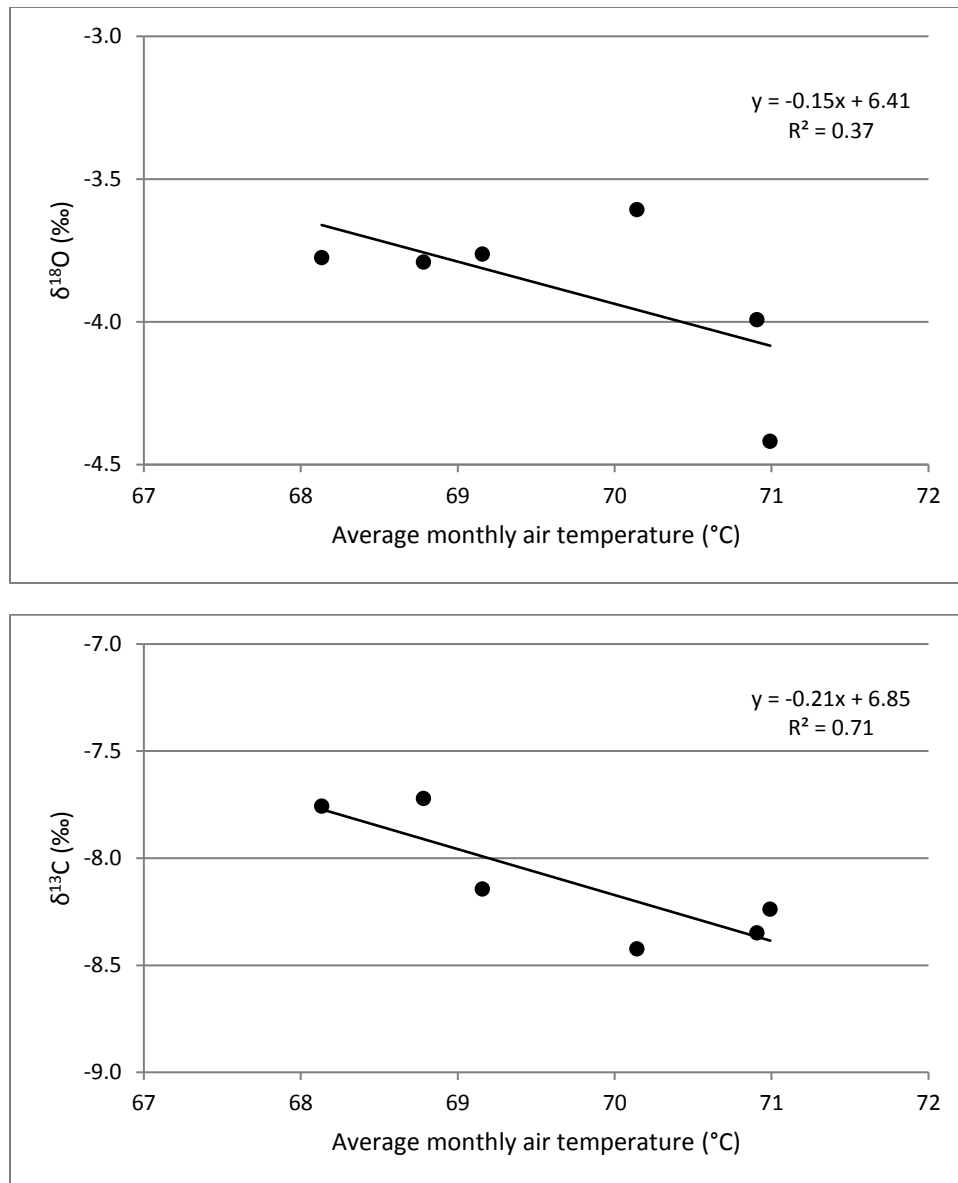


Figure 25. Relationships between annual average $\delta^{18}\text{O}$ (top) and $\delta^{13}\text{C}$ (bottom) in mussel shells and average monthly air temperature. The regression for $\delta^{13}\text{C}$ was statistically significant ($P = 0.04$), while the regression for $\delta^{18}\text{O}$ was not statistically significant.

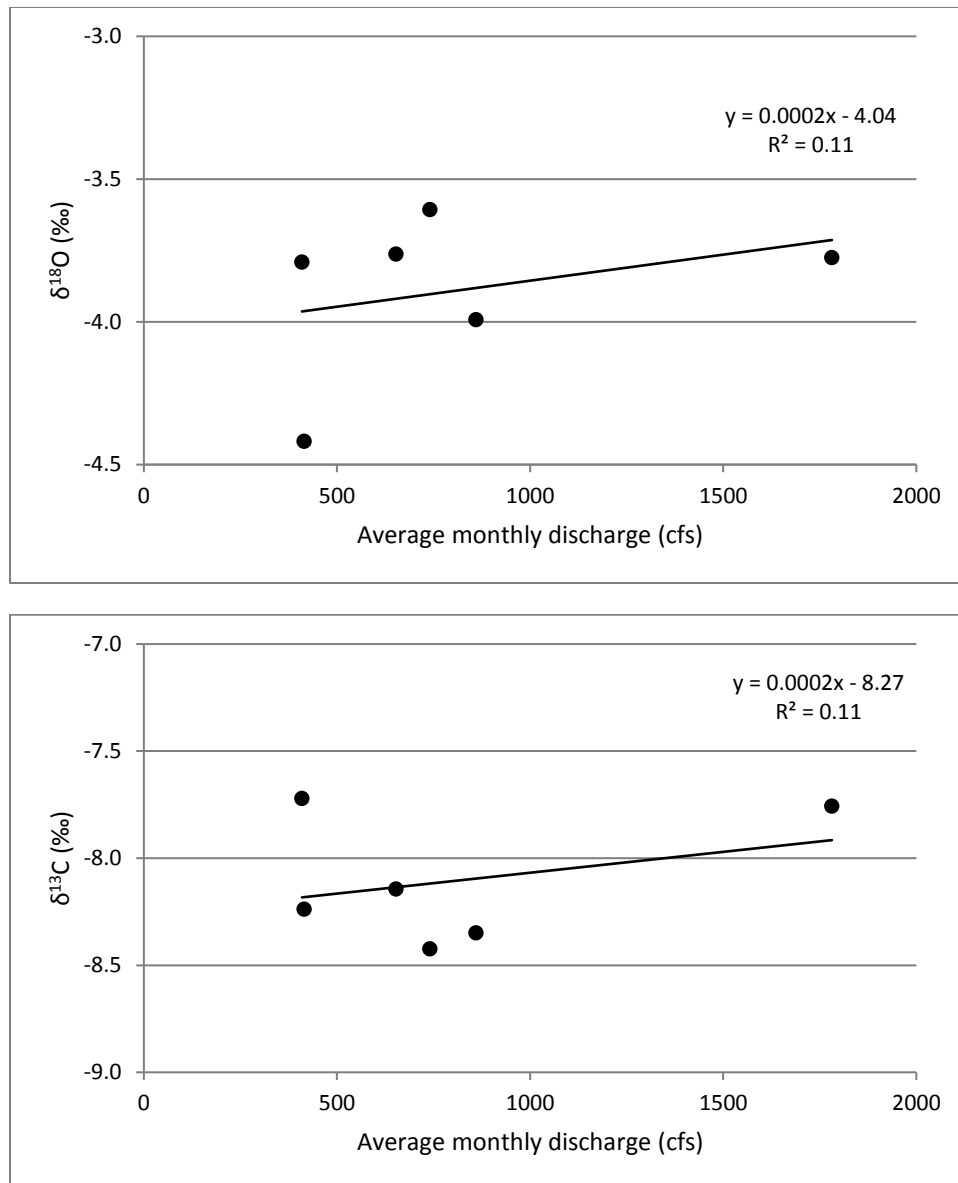


Figure 26. Relationships between annual average $\delta^{18}\text{O}$ (top) and $\delta^{13}\text{C}$ (bottom) in mussel shells and average monthly discharge (cubic feet per second) per year measured in the Guadalupe River at Gonzales, TX (USGS Station No. 08173900). Neither regression was statistically significant.

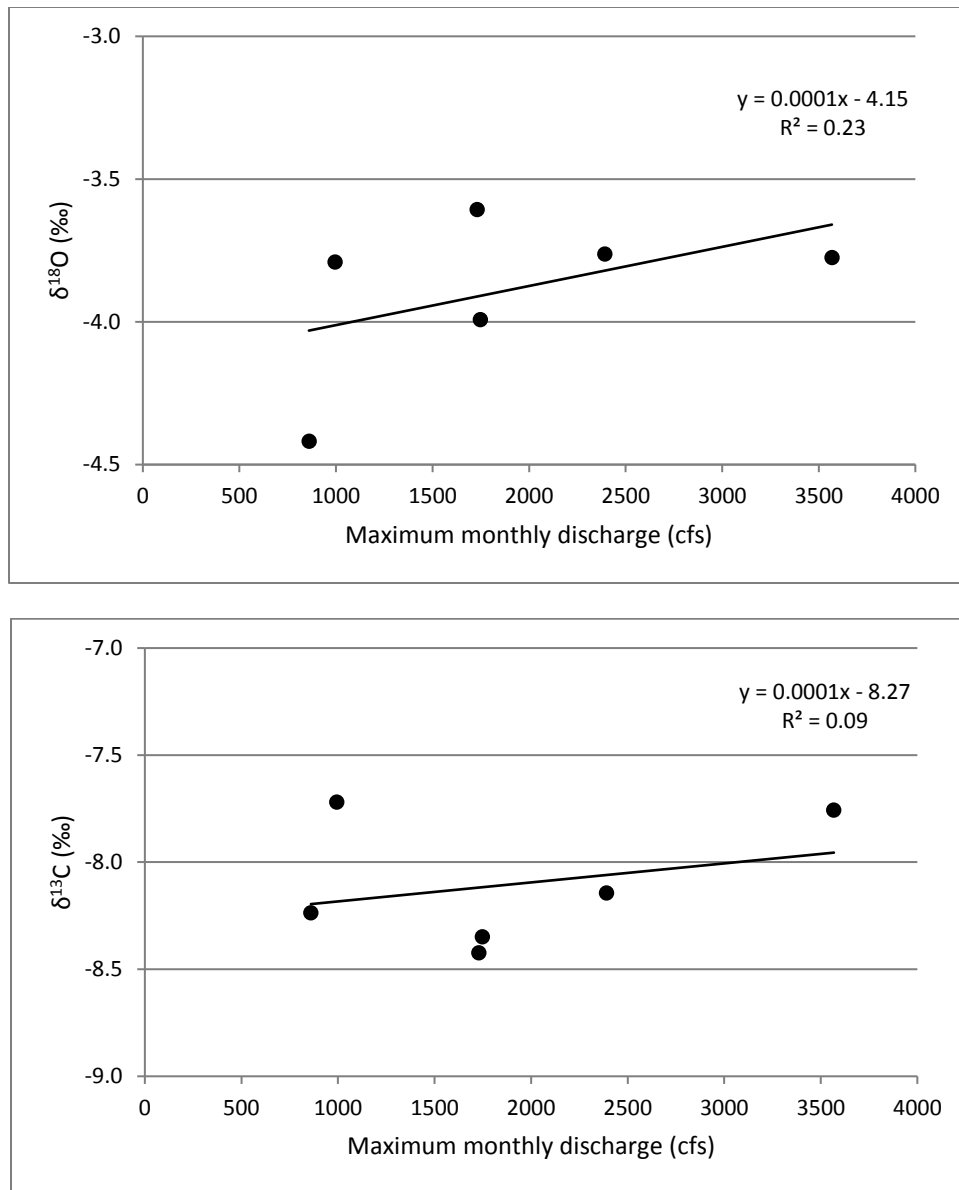


Figure 27. Relationships between annual average $\delta^{18}\text{O}$ (top) and $\delta^{13}\text{C}$ (bottom) in mussel shells and maximum monthly discharge (cubic feet per second) per year measured in the Guadalupe River at Gonzales, TX (USGS Station No. 08173900). Neither regression was statistically significant.

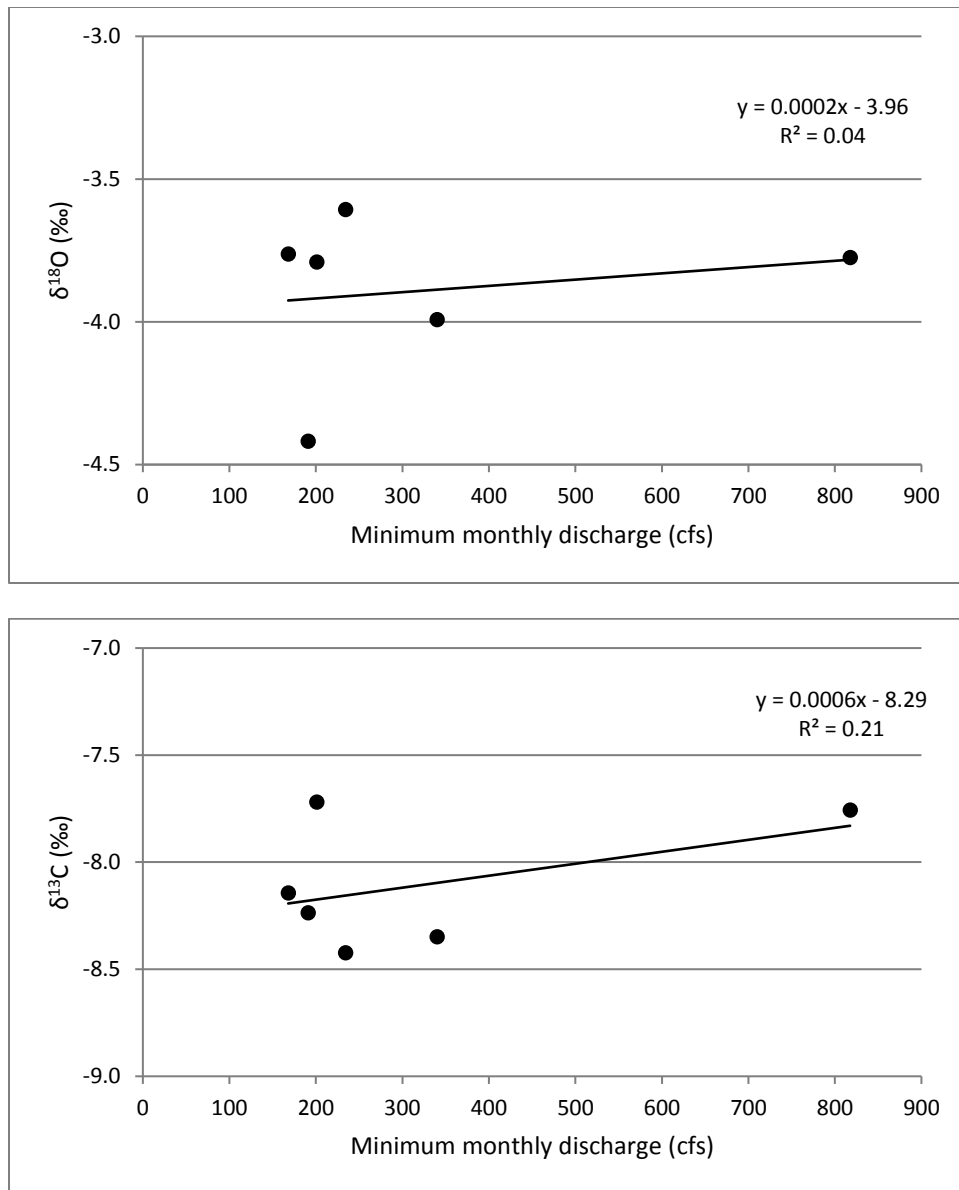


Figure 28. Relationships between annual average $\delta^{18}\text{O}$ (top) and $\delta^{13}\text{C}$ (bottom) in mussel shells and maximum monthly discharge (cubic feet per second) per year measured in the Guadalupe River at Gonzales, TX (USGS Station No. 08173900). Neither regression was statistically significant.

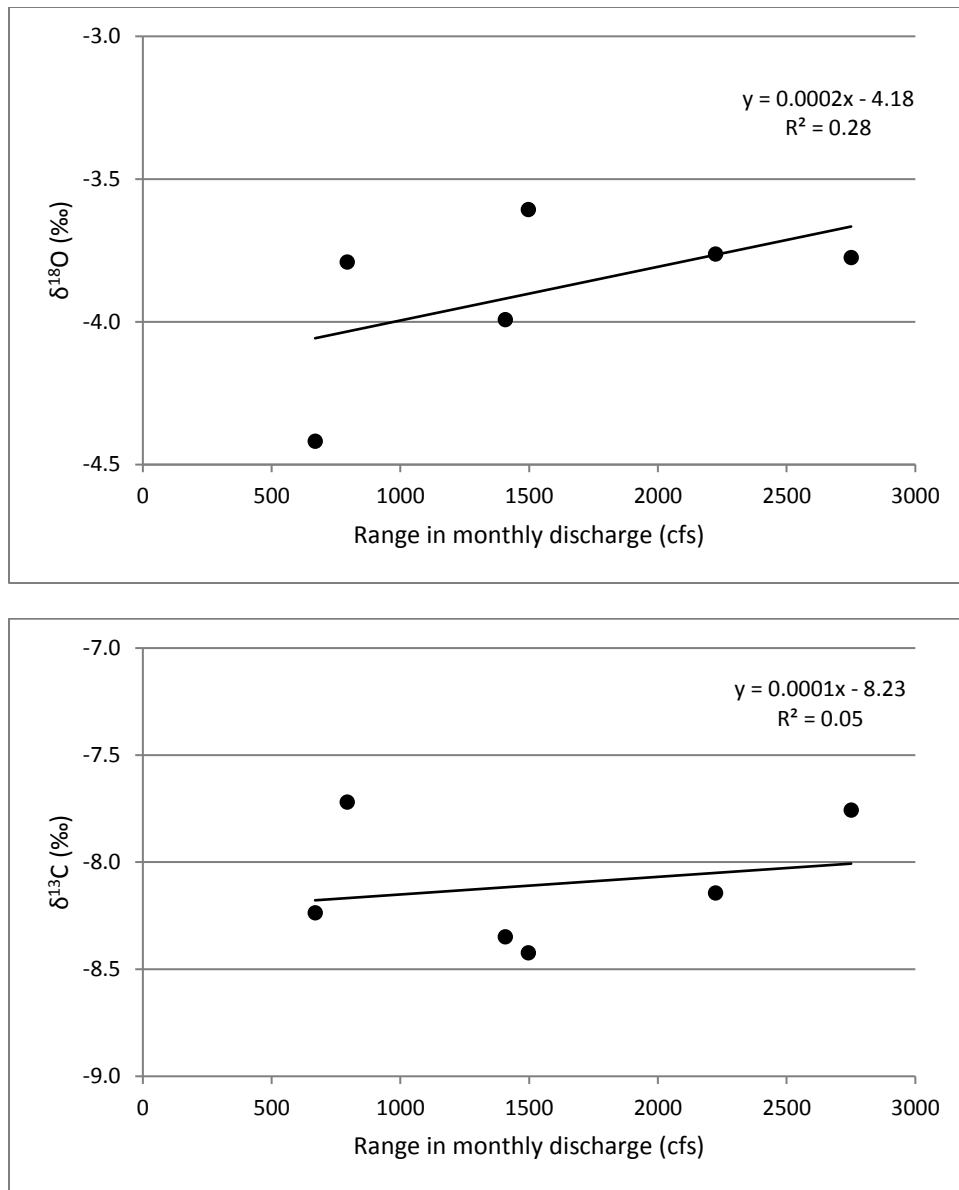


Figure 29. Relationships between annual average $\delta^{18}\text{O}$ (top) and $\delta^{13}\text{C}$ (bottom) in mussel shells and range (maximum minus minimum) monthly discharge (cubic feet per second) per year measured in the Guadalupe River at Gonzales, TX (USGS Station No. 08173900). Neither regression was statistically significant.

Acknowledgements

This project was funded by the Texas Parks and Wildlife Department and US Fish and Wildlife Service (jointly by State Wildlife Grant and Section 6 grant; ET-149-R). We also thank Nicholas Morin and Ryan Hladyniuk for their help in acquiring and analyzing freshwater mussel isotope samples.

References cited

- Black, B. A., J. B. Dunham, B. W. Blundon, J. Brim-Box, and A. J. Tepley. 2015. Long-term growth-increment chronologies reveal diverse influences of climate forcing on freshwater and forest biota in the Pacific Northwest. *Global Change Biology* **21**:594-604.
- Black, B. A., J. B. Dunham, B. W. Blundon, M. F. Raggon, and D. Zima. 2010. Spatial variability in growth-increment chronologies of long-lived freshwater mussels: Implications for climate impacts and reconstructions. *Ecoscience* **17**:240-250.
- Black, B. A., D. Griffin, P. van der Sleen, A. D. Wanamaker, J. H. Speer, D. C. Frank, D. W. Stahle, N. Pederson, C. A. Copenheaver, V. Trouet, S. Griffin, and B. M. Gillanders. 2016. The value of crossdating to retain high-frequency variability, climate signals, and extreme events in environmental proxies. *Global Change Biology* **22**:2582-2595.
- Corrège, T. 2006. Sea surface temperature and salinity reconstruction from coral geochemical tracers. *Palaeogeography, Palaeoclimatology, Palaeoecology* **232**:408-428.
- Cusack, M. and A. Freer. 2008. Biomineralization: elemental and organic influence in carbonate systems. *Chemical Reviews* **108**:4433-4454.
- Douglass, A. E. 1941. Crossdating in dendrochronology. *Journal of Forestry* **39**:825-831.
- Druffel, E. R. M. 1997. Geochemistry of corals: Proxies of past ocean chemistry, ocean circulation, and climate. *Proceedings of the National Academy of Sciences* **94**:8354-8361.
- Gillikin, D. P., K. A. Hutchinson, and Y. Kumai. 2009. Ontogenic increase of metabolic carbon in freshwater mussel shells (*Pyganodon cataracta*). *Journal of Geophysical Research* **114**:DOI: 10.1029/2008JG000829.
- Gillikin, D. P., A. Lorrain, S. Bouillon, P. Willenz, and F. Dehairs. 2006. Stable carbon isotopic composition of *Mytilus edulis* shells: relation to metabolism, salinity, $\delta^{13}\text{C}_{\text{DIC}}$ and phytoplankton. *Organic Geochemistry* **37**:1371-1382.
- Gillikin, D. P., A. Lorrain, L. Meng, and F. Dehairs. 2007. A large metabolic carbon contribution to the $\delta^{13}\text{C}$ record in marine aragonitic bivalve shells. *Geochimica et Cosmochimica Acta* **71**:2936-2946.
- Matta, M. E., B. A. Black, and T. K. Wilderbuer. 2010. Climate-driven synchrony in otolith growth-increment chronologies for three Bering Sea flatfish species. *Marine Ecology-Progress Series* **413**:137-145.
- McConnaughey, T. A., J. Burdett, J. F. Whelan, and C. K. Paull. 1997. Carbon isotopes in biological carbonates: Respiration and photosynthesis. *Geochimica et Cosmochimica Acta* **61**:611-622.

- McConnaughey, T. A. and D. P. Gillikin. 2008. Carbon isotopes in mollusk shell carbonates. *Geo-Marine Letters* **28**:287-299.
- Oczkowski, A. J., M. E. Q. Pilson, and S. W. Nixon. 2010. A marked gradient in $\delta^{13}\text{C}$ values of clams *Mercenaria mercenaria* across a marine embayment may reflect variations in ecosystem metabolism. *Marine Ecology Progress Series* **414**:145-153.
- Poulain, C., A. Lorrain, R. Mas, D. P. Gillikin, F. Dehairs, R. Robert, and Y. M. Paulet. 2010. Experimental shift of diet and DIC stable carbon isotopes: Influence on shell delta C-13 values in the Manila clam *Ruditapes philippinarum*. *Chemical Geology* **272**:75-82.
- Rypel, A. L., W. R. Haag, and R. H. Findlay. 2008. Validation of annual growth rings in freshwater mussel shells using cross dating. *Canadian Journal of Fisheries and Aquatic Sciences* **65**:2224-2232.
- Rypel, A. L., W. R. Haag, and R. H. Findlay. 2009. Pervasive hydrologic effects on freshwater mussels and riparian trees in southeastern floodplain ecosystems. *Wetlands* **29**:497-504.
- Sharp, Z. 2007. Principles of stable isotope geochemistry. Pearson Prentice Hall, Upper Saddle River, NJ.
- Strayer, D. L. 2008. Freshwater mussel ecology: a multifactor approach to distribution and abundance. University of California Press, Berkeley, CA.
- Strayer, D. L., J. A. Downing, W. R. Haag, T. L. King, J. B. Layzer, T. J. Newton, and S. J. Nichols. 2004. Changing perspectives on pearly mussels, North America's most imperiled animals. *BioScience* **54**:429-439.
- Surge, D., K. C. Lohmann, and D. L. Dettman. 2001. Controls on isotopic chemistry of the American oyster, *Crassostrea virginica*: implications for growth patterns. *Palaeogeography Palaeoclimatology Palaeoecology* **172**:283-296.
- Versteegh, E. A., H. Vonhof, S. Troelstra, and D. Kroon. 2011. Can shells of freshwater mussels (Unionidae) be used to estimate low summer discharge of rivers and associated droughts? *International Journal of Earth Sciences* **100**:1423-1432.
- Walther, B. D. and J. L. Rowley. 2013. Drought and flood signals in subtropical estuaries recorded by stable isotope ratios in bivalve shells. *Estuarine, Coastal and Shelf Science* **133**:235-243.
- Wanamaker, A. D., Jr., K. J. Kreutz, H. W. Borns, Jr., D. S. Introne, S. Feindel, S. Funder, P. D. Rawson, and B. J. Barber. 2007. Experimental determination of salinity, temperature, growth, and metabolic effects on shell isotope chemistry of *Mytilus edulis* collected from Maine and Greenland. *Paleoceanography* **22**:PA2217.

Wingard, G. L. and D. Surge. 2017. Application of molluscan analyses to the reconstruction of past environmental conditions in estuaries. Pages 357-387 *in* K. Weckström, K. M. Saunders, P. A. Gell, and C. G. Skilbeck, editors. Applications of Paleoenvironmental Techniques in Estuarine Studies. Springer Netherlands, Dordrecht.